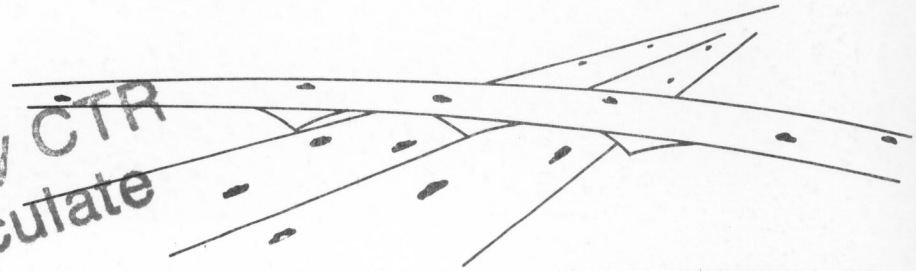

DEPARTMENTAL RESEARCH

Report Number 46-2

ANALYSIS OF STEEL STRESS AND CONCRETE MOVEMENT ON AN EXPERIMENTAL CONTINUOUSLY REINFORCED CONCRETE PAVEMENT

TEXAS HIGHWAY DEPARTMENT

ANALYSIS OF STEEL STRESS AND CONCRETE MOVEMENT

ON

AN EXPERIMENTAL

CONTINUOUSLY REINFORCED CONCRETE PAVEMENT

by

B. F. McCullough
Harvey J. Treybig

Research Report No. 46-2

Performance Study of
Continuously Reinforced Concrete Pavement
Research Project 1-8-63-46

Conducted By

Texas Highway Department
Highway Design Division, Research Section

In Cooperation With The
U. S. Department of Transportation
Federal Highway Administration
Bureau of Public Roads

May 1968

The opinions, findings, and conclusions expressed in this publication are those of the authors and not necessarily those of the Bureau of Public Roads.

A C K N O W L E D G M E N T S

The research reported herein was conducted under the supervision of Mr. M. D. Shelby, former Research Engineer, Mr. Robert L. Lewis, former Research Engineer, and under the general supervision of Mr. T. S. Huff, former Chief Engineer of Highway Design.

The authors wish to acknowledge contributions of Mr. A. C. Kyser, Houston Urban Engineer, whose farsightedness and cooperation made this study possible. Thanks is also extended to other members of the Houston Urban Office for the excellent cooperation throughout the various stages of this experimental project.

Special thanks is also given to Mr. Thomas F. Sewell and Mr. Fred C. Herber for their work which was instrumental in analyzing data, computer programming and preparation of this report.

Thanks are extended to Mr. W. J. Lindsay of the U. S. Bureau of Public Roads for his advice during the inception of this experimental project.

TABLE OF CONTENTS

LIST OF FIGURES

LIST OF FIGURES, Cont.

LIST OF TABLES

A B S T R A C T

An experimental continuously reinforced concrete pavement was built in Houston, Texas, in 1964. It was experimental in the sense that it had varying percentages of longitudinal reinforcement and also varying preformed crack spacings. Data taken included strains in the longitudinal steel as measured with electrical strain gages, concrete movement as measured by mechanical strain gages, surveys of the crack spacing with time, and a continuous temperature recording of the slab temperature. These data were analyzed and empirical equations have been developed for steel stress and crack width in the concrete.

Some of the parameters which are displayed in the stress and crack width equations are the thermal coefficient of expansion of the concrete, temperature change in the slab, modulus of elasticity of the concrete , the crack spacing in the concrete, the percentage of longitudinal steel reinforcement and the shrinkage of the concrete.

ANALYSIS OF STEEL STRESS AND CONCRETE MOVEMENT ON AN EXPERIMENTAL CONTINUOUSLY REINFORCED CONCRETE PAVEMENT

I. INTRODUCTION

Background

This report is part of a continuing study by the Texas Highway Department pertaining to the performance and design study of continuously reinforced concrete pavement.[1,2,3,4,5,6] From a design standpoint there is a considerable lack of information as to how much longitudinal steel should be used in continuously reinforced pavement. Texas has been using 0.5 per cent in most of their designs. This percentage seems to be performing quite well at the present, but there may be a possibility of using less to make a more economical pavement. Therefore, this experimental study was initiated to see what effect per cent longitudinal steel had on the stresses which would arise.

Scope

In order to establish the effect of the per cent longitudinal steel and a varied crack spacing, an experimental project was set up in Houston, Texas. The project was laid out employing various percentages of longitudinal reinforce-

ment, various crack spacings and two different coarse aggregate types to create two different moduli of elasticity concretes. The purpose of the full scale experiment was to determine and evaluate variations in: (1) strains in the concrete and steel, (2) crack pattern, (3) crack widths due to variations in longitudinal steel percentages, (4) crack spacings, and (5) climatic conditions.

Other objectives of this study were: (1) to develop an empirical equation to predict steel stress, and (2) to develop an empirical equation to predict crack width in the concrete.

II. EXPERIMENT DESIGN AND PROCEDURES

Location and Layout

The test location was selected by considering many factors. Among these were general area, type of soil, traffic conditions, timing, test control and need for test information. The test area chosen is located in Houston, Texas, and is the frontage road to Interstate Highway 610, Figure 2.1. One test area is located on the north frontage street from Long Drive in an easterly direction for a distance of 1,700 feet and consists of standard aggregate continuously reinforced concrete pavement. The second test area is located on the south frontage street extending from South Wayside Drive in an easterly direction for 900 feet and consists of lightweight continuously reinforced concrete pavement.

Figure 2.2 depicts the general layout of the test area by station number, test areas, and transition areas. Each of the test sections are 200 feet long with transition sections 100 feet long where the percentage of steel was changed. The standard concrete and lightweight concrete were placed near enough to one another to reduce differences in environmental condition to a very minimum.

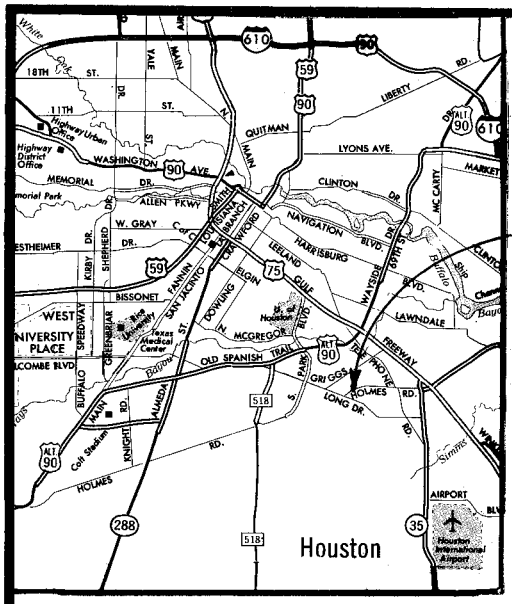

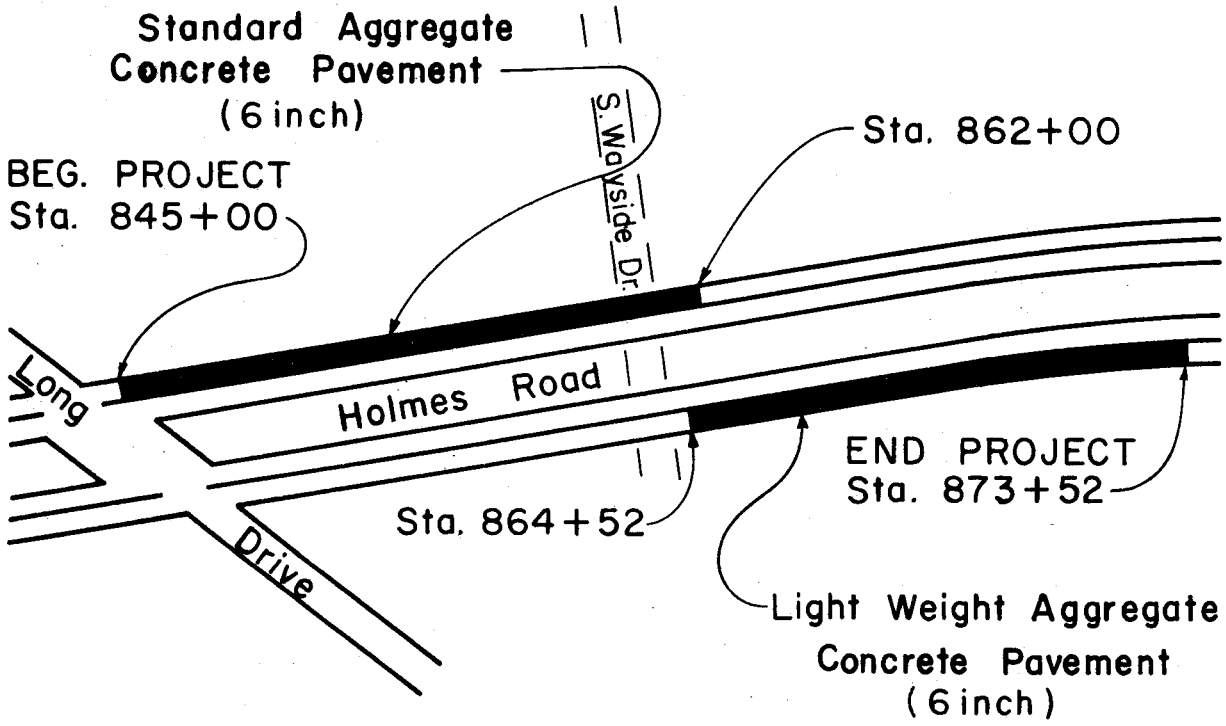

LOCATION AND LAYOUT OF HARRIS COUNTY PROJECT

Fig. 2.1

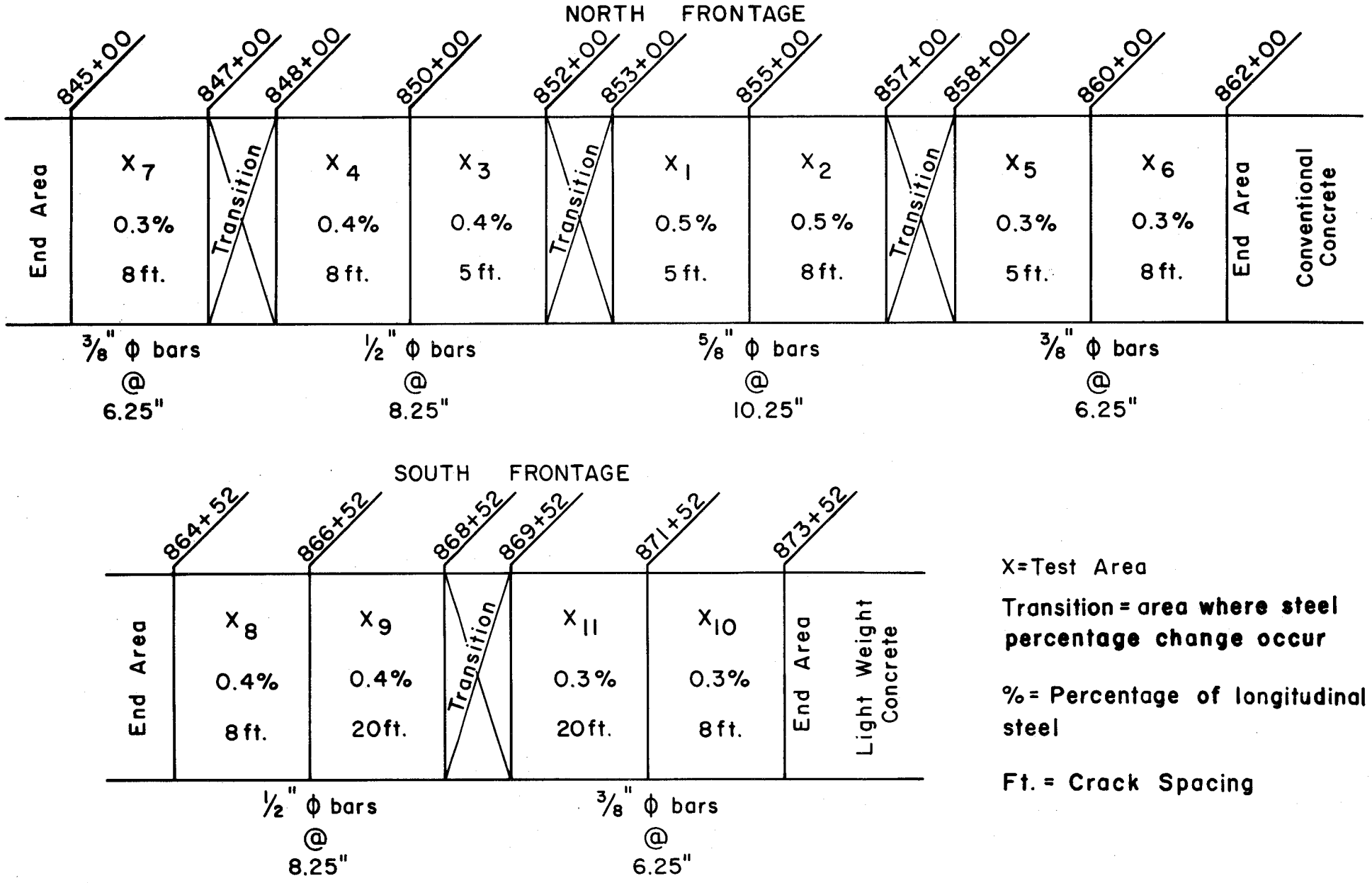

TEST AREA LAYOUT FOR HARRIS COUNTY PROJECT

Figure 2.2

The locations of each of the test sections were randomized with respect to steel percentage. Full randomization was not possible due to construction problems and available slab length. The location of the test sections for any given percentage of steel were randomized with respect to crack spacing.

In general, the terrain consists of a flat plain with black clayey soil. Each test slab has two lanes, and in each the traffic is uni-directional. A typical section for a frontage road on the project is shown in Figure 2.3. Where a third lane was added it was not a part of the test area. The top six inches of subbase material is cement stabilized oyster shell. The pavement has a six-inch curb. The test slabs are uniform six-inch slabs placed in monolithic 22-foot and 24-foot pours.

Steel Design. The project had 0.3 per cent,* 0.4 per cent, and 0.5 per cent longitudinal reinforcing steel in the standard CRCP and 0.3 per cent and 0.4 per cent steel in the lightweight CRCP. Five-tenths per cent steel was not used in the lightweight CRCP for theoretical reasons. Complete randomization of test sections was not used due to construction problems and length of project. Table 2.1 shows the steel stress experiment factorial.

*Ratio of cross sectional area of the steel to the concrete area.

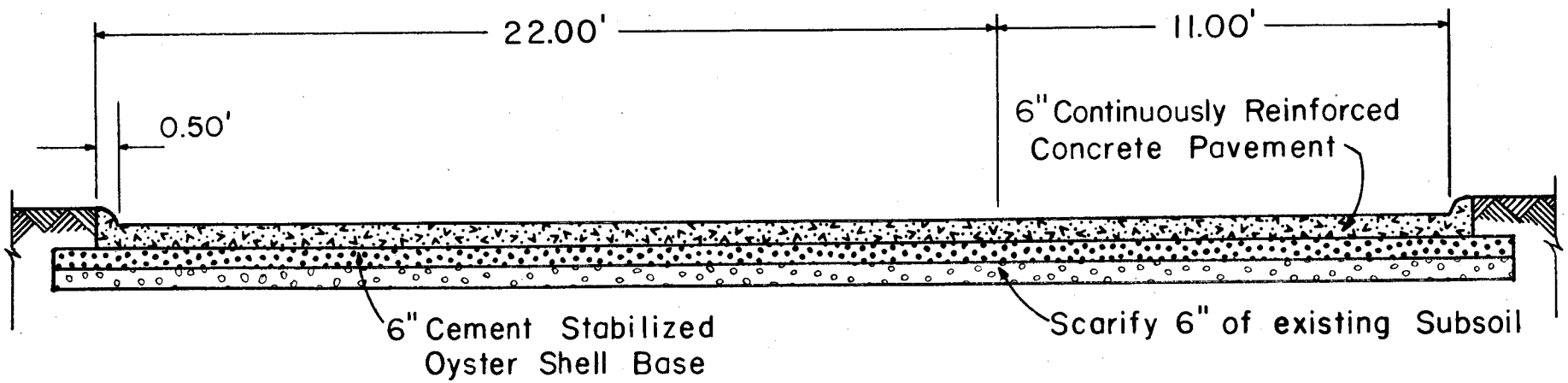

TYPICAL SECTION FOR HARRIS COUNTY PROJECT

Figure 2.3

TABLE 2.1

EXPERIMENTAL FACTORIAL DESIGN

Pavement Type / % Steel / Crack Spacing	Conventional			Lightweight	
	0.3	0.4	0.5	0.3	0.4
5'	5	3	1		
8'	6&7	4	2	10	8
20'				11	9

The longitudinal steel for the 0.5 per cent design consisted of 5/8 inch bars at 10 1/4 inch centers, 0.4 per cent design consisted of 1/2 inch bars at 8 1/2 inch centers, and 0.3 per cent design consisted of 3/8 inch bars at 6 1/4 inch centers. While the designs are referred to as the 0.5 per cent, 0.4 per cent, and 0.3 per cent, the actual percentages are 0.504, 0.404, and 0.293, respectively. On both designs, lightweight and standard, the transverse steel consisted of 1/2 inch bars at 32 inch centers. The bond area to volume of concrete ratios for the 0.5, 0.4 and 0.3 designs were 55.7, 54.8 and 55.3 $\frac{in\ 2}{ft\ 3}$ respectively.

Concrete Design. The standard CRCP was designed in accordance with Item 366 of the Standard Specifications which requires a minimum flexural strength* of 575 psi.(7)

The specifications for lightweight concrete called for a flexural strength and modulus of rupture of not less than 500 pounds per square inch at the age of seven days. The specifications for the concrete are shown in Table 2.2 below:

SPECIFICATIONS FOR LIGHTWEIGHT CONCRETE

Cement Ratio	Air Content	Slump	Lightweight Aggregate	Unit Weight	Fine Aggregate
5 1/2 sacks per C.Y.	6%-9% by Volume	2-3 In.	ASTM, C330	No More Than 55 Lbs. per Cu. Ft.	Natural Sand

Table 2.2

* Mid-point loading.

In both the standard CRCP and the lightweight CRCP, the design was such to encompass what was considered as an optimum crack spacing. To obtain these different crack spacings, the design called for preformed cracks. These preformed cracks were provided for by placing corrugated sheet metal strips four inches high across the width of the pavement at predetermined distances. These sheet metal strips were fabricated from thin gage galvanized sheet metal. The corrugated strips were notched below each strain gage for installation purposes.

Terminal Treatment. In addition to the normal expansion joint on the west end of the north frontage road, the pavement end was anchored by means of two transverse lugs to limit end movement.[6]

Instrumentation

In the design of the instrumentation layout, precautions were taken to assure ease of the installation, optimum performance, and that representative data would be obtained.

The general layout of the instrumentation is shown in Figure 2.4. All instrumentation was placed in the outside lane and centered in each quarter section of the lane.

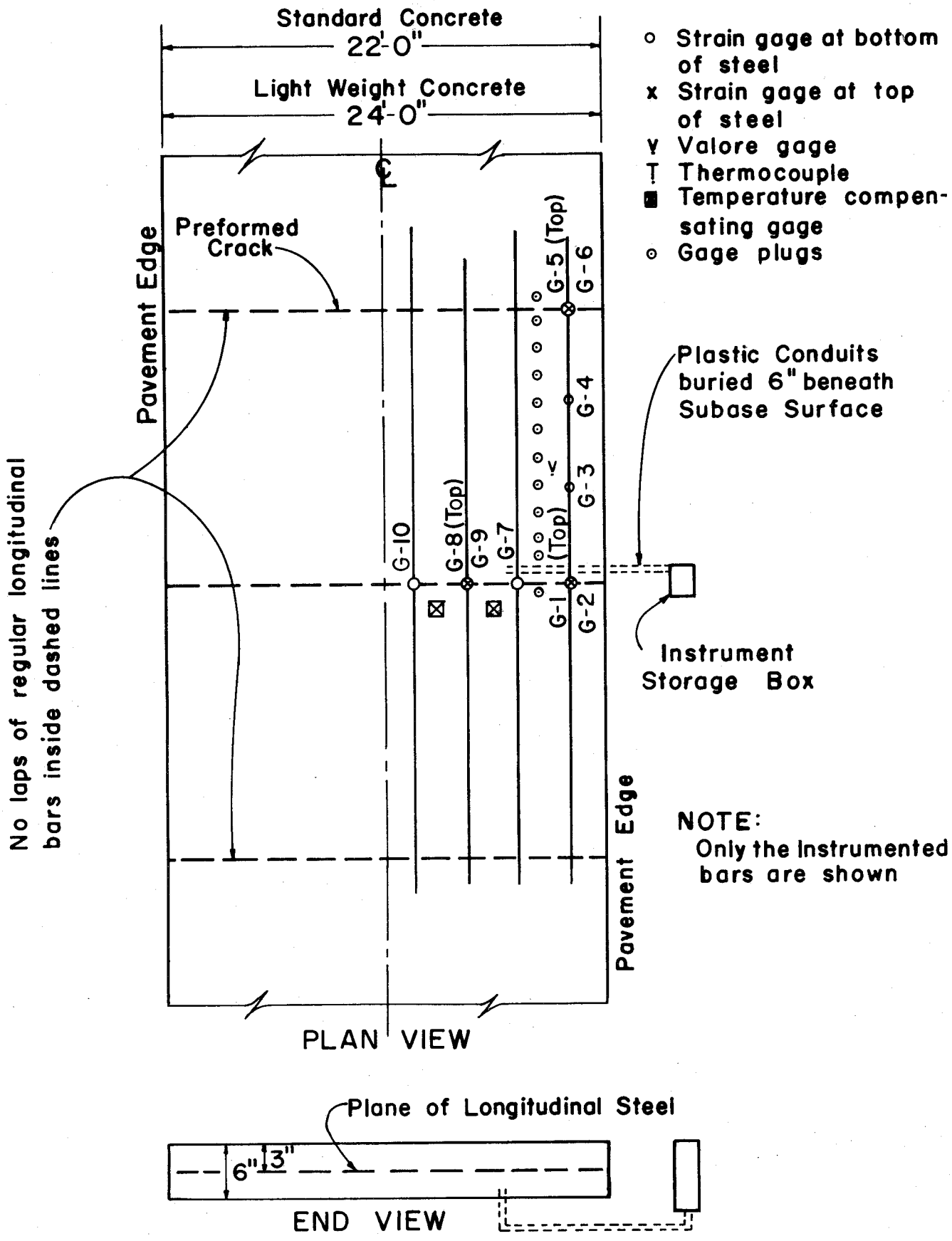

GENERAL LAYOUT OF HARRIS COUNTY INSTRUMENTATION TEST AREA

FIGURE 2.4

All leads for a test section were brought to a storage box at the right of way line by plastic conduits that were placed six inches beneath the surface. The instrumentation storage containers are sections of pipe appropriately provided with lock as shown in Figure 2.5. Electrical power for the instrumentation was provided by a small unit mounted on a truck. This mobile unit and voltmeter could be moved to each test section. Ten strain gages were used in each test section. Figure 2.4 shows the position of strain gages relative to one another, and to the preformed cracks. The gages were positioned in such manner that the longitudinal strain distribution along the bar and transverse strain distribution at the crack could be determined, Figure 2.6.

Provisions for measuring concrete movement were made by placing brass gage plugs two inches long and one-half inch in diameter in the surface of the concrete at ten-inch centers as shown in Figure 2.7.

The number of plugs inserted in each test area varied in accordance with the crack spacing. The plugs were spaced ten inches apart and in a relative position to the test instrumentation as shown in Figure 2.4.

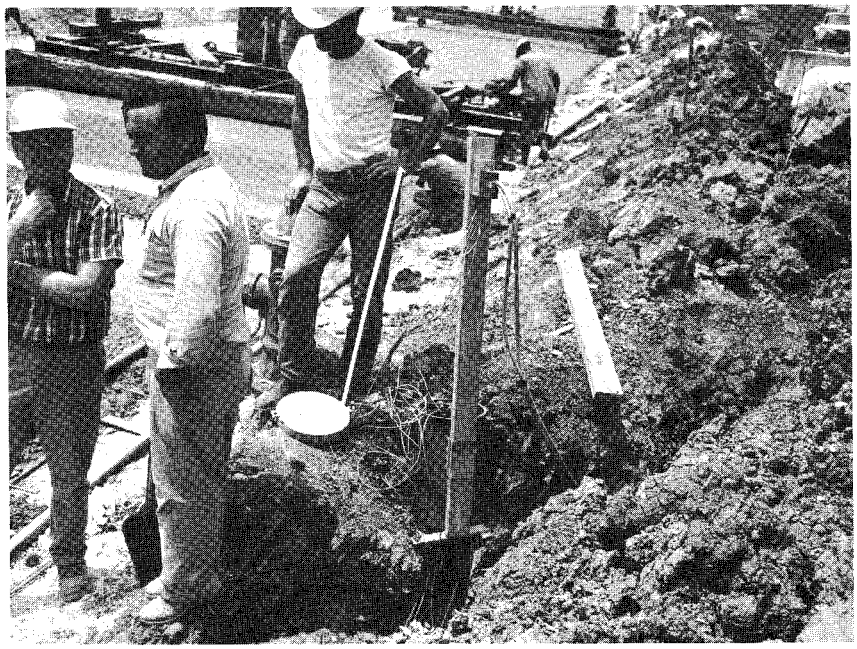

FIGURE 2.5
Instrument Storage Container

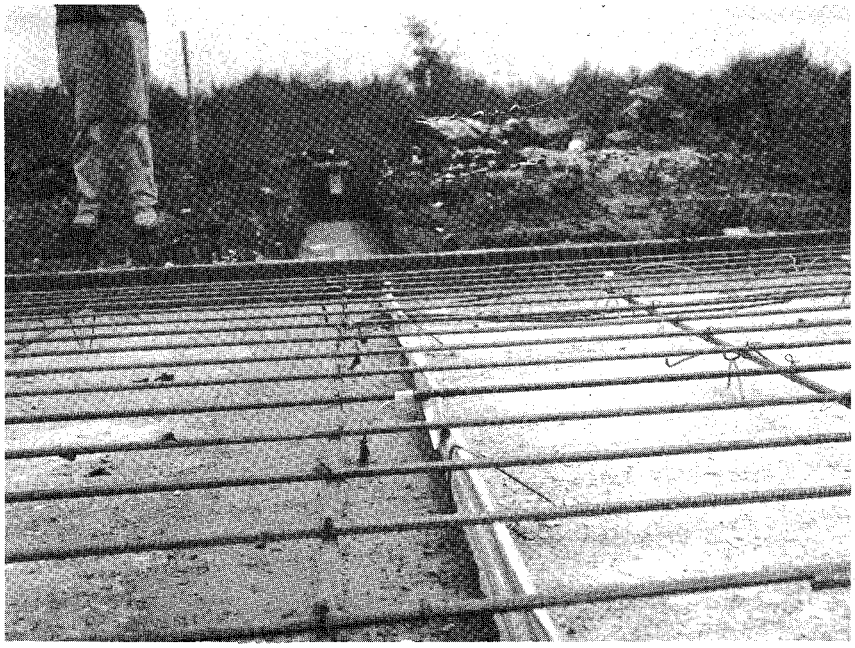

FIGURE 2.6
Strain Gage Installation

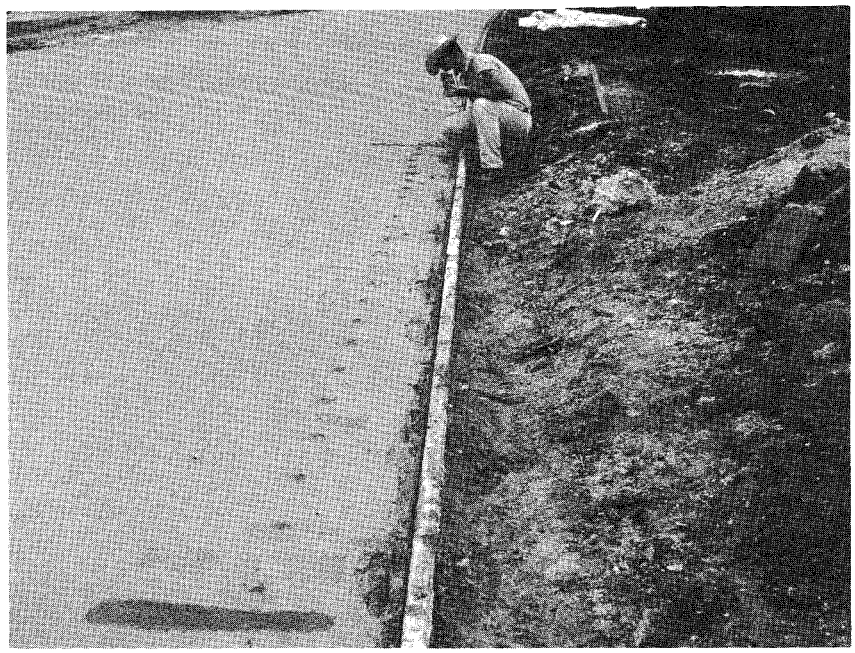

FIGURE 2.7
Setting Gage Plugs

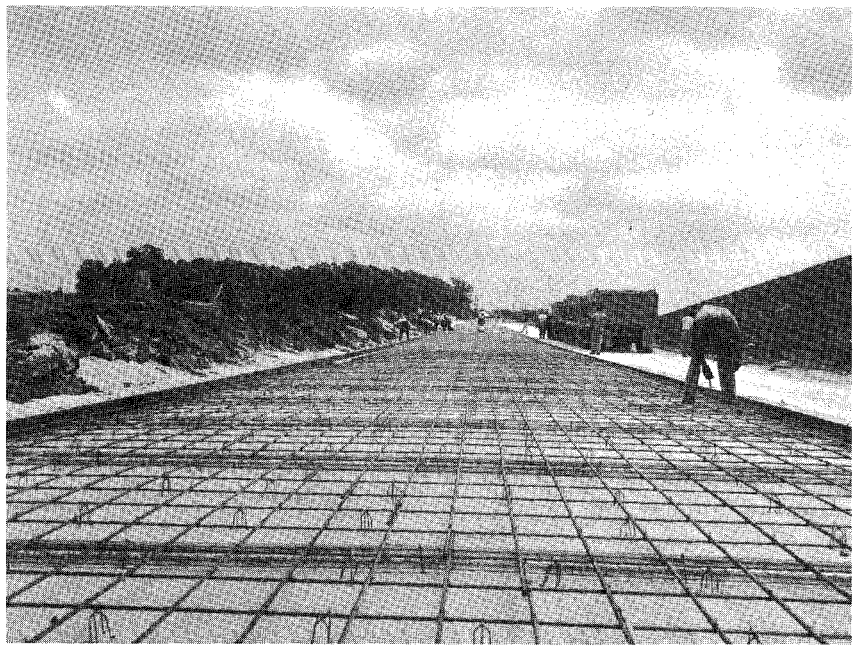

FIGURE 2.8
Construction for Preformed Cracks

One thermocouple was installed in each test area to record temperatures by a change in voltage on the Digital Voltmeter. Three resistance thermometers were installed at a selected location in the lightweight section, one located one-half inch from the surface, one in the center, and one one-half inch from the bottom. The resistance thermometers were installed to determine the variation of temperature from top to bottom in the lightweight pavement.

Construction

In order to minimize the effect of differential weather conditions, the specifications required that each of the two slabs be placed in one working day. All the test sections with standard CRCP were placed in one day, and those with lightweight CRCP were placed ten days later. Section 6 and its replicate, Section 7, were placed at opposite ends of the conventional slab to evaluate any possible effect of differential curing temperatures. The contractor was required to delay 14 days between the placement of the test slabs and the placement of third lane. Paving operations were accomplished by Brown & Root Construction Company of Houston.

The unique feature of this operation was the pre-forming of the transverse cracks. Preformed cracking was

provided for in each test section by placing thin gage, galvanized and corrugated sheet metal four inches high across the width of the pavement at predetermined distances as shown in Figure 2.8. Figures 2.9 through 2.13 show some general views of the various phases of construction and installation of equipment.

Each of the test slabs was placed continuously and in one working day. The standard concrete was placed from west to east on May 8, 1964. The weather was clear and sunny, and the time and temperature for placing each test area were as follows:

Test Area	Time	Temperature (^{o}F)
7	0635	77
4	0750	80
3	1015	80
1	1037	83
2	1130	82
5	1315	86
6	1416	91

The lightweight concrete was placed May 14, 1964, a typical cloudy hot day, with a short downpour of rain during the placement of test areas 10 and 11. The time and temperature for placing each test area were as follows:

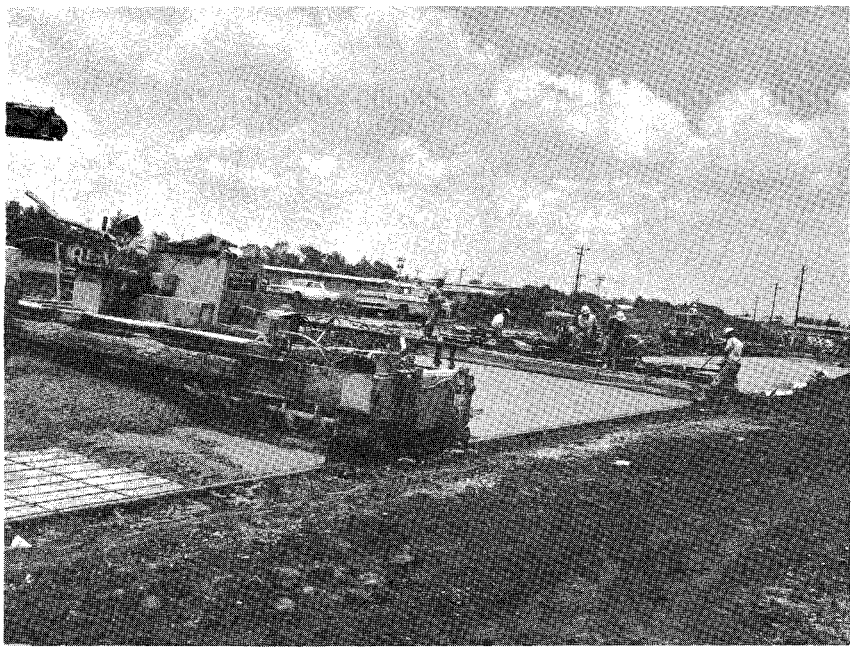

FIGURE 2.9
Paving Train in Operation

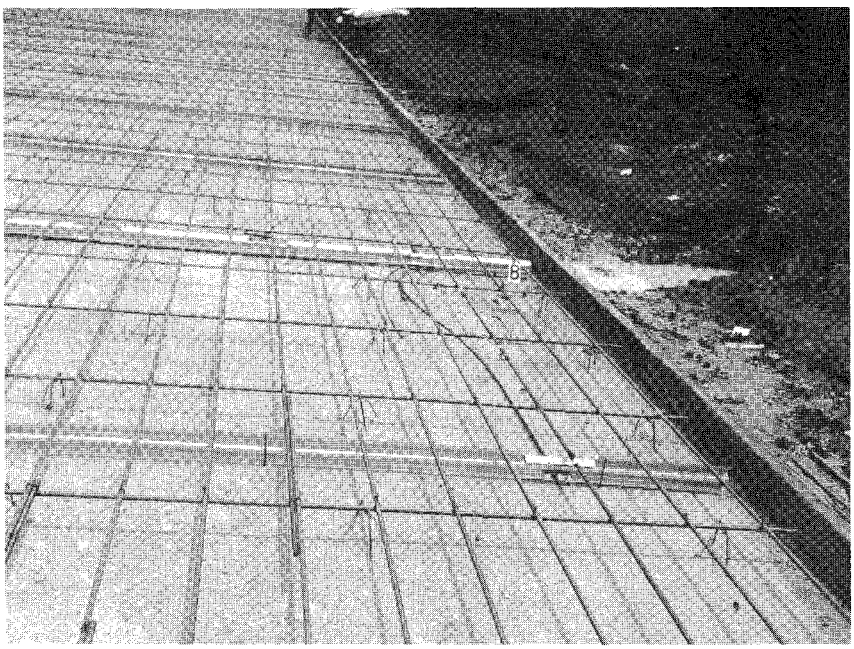

FIGURE 2.10
Steel and Crack
Spacers in Place

FIGURE 2.11
Paving Operations in Progress

FIGURE 2.12
Placing Concrete

Test Area	Time	Temperature (^{o}F)
10	1208	84
11	1219	84
9	1306	87
8	1420	91

Testing

Field testing procedures for this project were worked out as near as possible prior to the initiation of field testing. This was necessary, because after field testing began there was no time to work out such matters since the concrete properties change drastically during the first few days and much valuable data would be lost by any delay.

Steel Modulus of Elasticity. Before the steel was placed, several tests were performed on specimens to determine the modulus of elasticity. Tests were performed using a mechanical strain gage and then replicate measurements were made using electrical strain gages. Very close correlation was obtained in this procedure. It was found that a modulus of 30.2×10^{6} psi should be used for the steel on this project. Appendix A covers the determination of the modulus of elasticity of the steel.

Concrete Properties. Testing for concrete properties was conducted by the Materials and Tests Division of the

Texas Highway Department under laboratory conditions as no field testing equipment was readily available. It should be pointed out, however, that the test molds were made in the field and consisted of on-the-site concrete. Appendix B covers the laboratory testing conducted for the experimental CRCP.

Field Data. For the first eight days concrete movement, steel stress and temperature data were taken on all eleven sections every two hours. Afterward periodic readings were taken at times when temperature and strain readings were changing most drastically.

To obtain measurements the mobile unit, which was equipped with an electrical power plant and voltmeter, was driven to each test site. This mobile unit is shown in Figure 2.14. The instrumentation could then be plugged into the junction box at each test site and steel stress, concrete movement, and temperature readings could be taken and recorded. Concrete movement was measured by the use of a Soil Test Mechanical Strain Gage which detects movement to the 0.0001 of an inch.

The strains in the steel were determined by use of waterproofed SR-4 electrical strain gages. Strain readings

FIGURE 2.13
Covering Instrumentation with
Concrete Ahead of General Operations

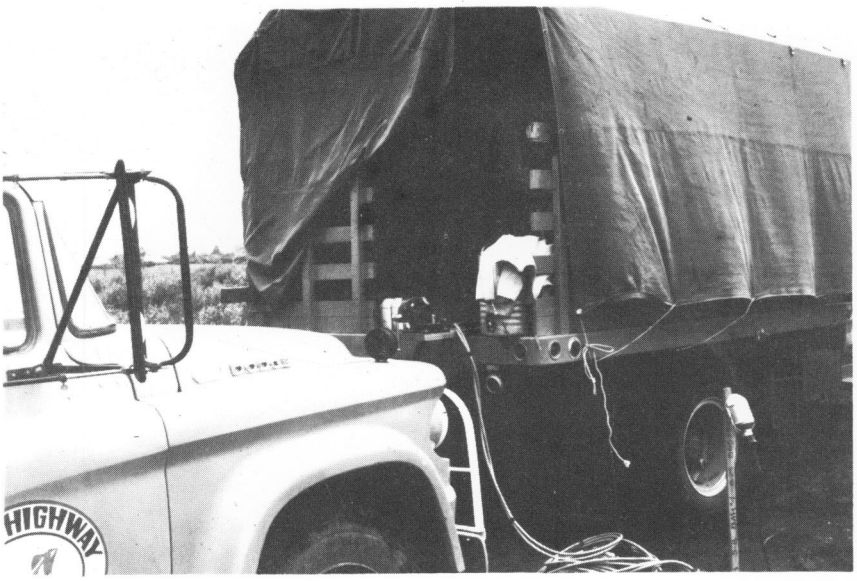

FIGURE 2.14
Truck in Operation

were taken by using a Beckman Digital Voltmeter in an unbalanced Wheatstone Bridge circuit capable of resolving 10×10^{-6} volts. The Model 910-VR Voltmeter-Ratiometer was used with voltage measurement ranges from $\pm$00.001/19.990/-199.90, 1100.0 to obtain temperature measurements. Ice water was used as a standard temperature reference.

All field data were recorded on special forms, to facilitate keypunching computer cards for analysis of the data. These data forms are shown in Appendix E.

III. BASIC STUDIES

Before the field data taken on this project could be used in an analysis, the data had to be converted to values that would be useful. Also the concrete properties obtained in the laboratory had to be expanded to include all days of field testing so that comparison studies could be conducted.

Converting Digital Voltmeter Readings Into Stress

Strain readings taken by use of the digital voltmeter and an unbalanced Wheatstone Bridge circuit were converted to steel stress by the use of the following equation:

$$S = \frac{4E}{VFK} (e_n - e_o)$$

Where:

S = steel stress, psi

e = voltmeter readings, (V x 10 x 10^{-6} accuracy)

E = modulus of elasticity for reinforcing steel, (30.2 x 10^6) psi

V = line voltage (4.804 volts)

K = correction factor for strain gages (0.970833)

F = gage factor of strain gage

From the above equation, it was found that the stress in the steel was to an accuracy of ±123 psi.

Concrete Movement Calculations

Longitudinal concrete movement was measured with a ten inch multi-position strain gage. Brass plugs with holes, 1/16 inch in diameter and 1/8 inch deep, drilled in their tops were inserted in the concrete for measuring points. With the strain gage used, movements as small as one-ten thousandths of an inch (0.0001") were detected. The recorded data is translated to relative movement as follows:

$$C = A - B \quad \ldots\ldots\ldots\ldots\ldots (1)$$

Where:

A = reading with the strain gage on the standard bar

B = reading with the strain gage on adjacent plugs in the pavement

C = relative movement between adjacent gage plugs

The values from Equation (1) are then substituted into the following equation:

$$X_G = C_n - C_o \quad \ldots\ldots\ldots\ldots\ldots (2)$$

Where:

X_G= movement experienced between adjacent gage plugs after the reference readings, inches

C_o= initial or base difference, inches (Zero reading)

C_n= difference at any interval after the base difference, inches

Movement is used in lieu of strain in this investigation since any measured movement is not due to strain of the concrete but to relief from restraint stresses developed due to suppressed volume changes of the concrete. (8) In other words, if no movement was recorded after a temperature drop, then restraint stresses are developed in the slab. Any movement of the slab segment is relief from the restraint stresses.

Development of Intermediate Concrete Modulus of Elasticity, Shrinkage, and Thermal Coefficient Data

The concrete properties data for this project were taken at four different periods of the first 28 days. However, if other field data in between these four periods

were to be compared with these properties, more intermediate data would be needed. Table 3.1 shows the concrete properties obtained for 3, 7, 14 and 28 days for the conventional concrete sections and Table 3.2 shows lightweight concrete sections.

A detailed study was made of earlier experiments[9,10] in comparing concrete properties as a function of age and weather. From this study a set of data for concrete properties was derived encompassing the days for this analysis. Table 3.3 shows the concrete properties for the conventional sections and Table 3.4 shows the concrete properties for the lightweight sections.

Crack Pattern Investigation

One of the main objectives of this experiment was the study of different combinations of crack spacing and per cent steel and to attempt to evaluate any optimum crack spacing pattern that might exist.

Crack Surveys. The standard CRCP and lightweight CRCP were placed May 8, 1964, and May 18, 1964, respectively. These pavements were under close observation since that time so that any change in crack spacing has been recorded and evaluated. Crack surveys were made at selected

CONCRETE PROPERTIES OF STANDARD CRCP

	NUMBER OF DAYS AFTER PLACEMENT			
	3	7	14	28
Compressive Strength (psi)	2367	3329	4126	4313
Tensile Strength (psi)	317	344	442	488
Modulus of Elasticity (Compression)	4.47×10^6	5.65×10^6	6.16×10^6	7.23×10^6
Flexural Strength (psi)	534	661	659	643
Bond Strength (psi)	827	1029	1282	1206
Shrinkage (in/in)	-	9.05×10^{-5}	12.7×10^{-5}	12.7×10^{-5}
Thermal Coeff. (in/in/^{o}F)	-	-	-	6.04×10^{-6}

Table 3.1

CONCRETE PROPERTIES OF LIGHTWEIGHT CRCP

	NUMBER OF DAYS AFTER PLACEMENT			
	3	7	14	28
Compressive Strength (psi)	1483	2369	3208	3828
Tensile Strength (psi)	238	284	275	312
Modulus of Elasticity (compression)	1.91×10^6	2.30×10^6	2.78×10^6	2.96×10^6
Flexural Strength (psi)	407	526	609	607
Bond Strength (psi)	694	893	871	1011
Shrinkage (in/in)	-	0	11.32×10^{-5}	20.38×10^{-5}
Thermal Coeff. in/in/^{o}F.	-	-	-	5.03×10^{-6}

Table 3.2

DATE	AGE (DAYS)	SHRINKAGE	MODULUS OF ELASTICITY (10^6 psi)	THERMAL COEFFICIENT
5-8-64	1	3	3.12	4.40
5-9-64	2	38	4.00	5.70
5-10-64	3	80	4.51	5.90
5-11-64	4	60	4.87	6.06
5-12-64	5	56	5.13	6.15
5-13-64	6	84	5.37	6.24
5-14-64	7	106	5.56	6.30
5-15-64	8	118	5.72	6.34
	9	110	5.87	6.35
	10	100	6.00	6.36
5-18-64	11	92	6.11	6.35
5-19-64	12	86	6.23	6.35
5-20-64	13	83	6.32	6.32
5-21-64	14	82	6.41	6.30
5-22-64	15	85	6.50	6.26
5-23-64	16	88	6.58	6.22
5-24-64	17	88	6.65	6.19
5-25-64	18	87	6.72	6.15
	19	85	6.79	6.12
	20	83	6.85	6.11
	21	80	6.91	6.08
	22	79	6.97	6.06
	23	77	7.02	6.05
	24	76	7.08	6.03
	25	75	7.13	6.01
6-2-64	26	75	7.18	6.00
6-3-64	27	75	7.22	6.00
10-29-64	174	220	7.50	5.90
1-12-65	249	220	7.50	5.90
1-27-65	264	220	7.50	5.90
3-31-65	327	220	7.50	5.90
6-1-65	388	220	7.50	5.90

Table 3.3

REVISED CONCRETE PROPERTIES FOR
STANDARD CONCRETE SECTIONS

DATE	AGE (DAYS)	SHRINKAGE	MODULUS OF ELASTICITY (10^6 psi)	THERMAL COEFFICIENT
5-18-64	1	24	1.47	3.40
5-19-64	2	41	1.78	4.70
5-20-64	3	46	1.91	4.90
5-21-64	4	38	2.10	5.06
5-22-64	5	44	2.20	5.16
5-23-64	6	43	2.28	5.24
5-24-64	7	32	2.30	5.30
5-25-64	8	12	2.41	5.34
5-26-64	9	16	2.46	5.35
	10	32	2.50	5.36
	11	48	2.52	5.35
	12	70	2.55	5.34
	13	86	2.57	5.32
	14	104	2.78	5.30
	15	122	2.60	5.26
6-2-64	16	140	2.62	5.22
6-3-64	17	160	2.64	5.19
10-30-64	164	650	3.00	4.90
1-12-65	239	720	3.00	4.90
1-27-65	254	722	3.00	4.90
3-31-65	317	737	3.00	4.90
6-1-65	378	737	3.00	4.90

Table 3.4

REVISED CONCRETE PROPERTIES FOR
LIGHTWEIGHT CONCRETE SECTIONS

intervals since the initial placement of the concrete. Graphs showing average crack spacing versus age in days are shown in Figures 3.1 and 3.2 and the results are shown in tabular form in Tables 3.5 and 3.6. The average crack spacing is obtained by dividing the length of the test section under consideration by the number of cracks within the test section.

Standard CRCP Sections. Inspection of Figure 3.1 indicates that the standard CRCP crack pattern had reached a near stable condition during the first four days after placement, with the exception of Sections 5 and 7 which took eighteen and sixteen days, respectively. It should also be noted that after 201 days, the conventional concrete sections continued to crack on a limited extent with the exception of Sections 5 and 6. The additional cracking may be explained by the additional contraction stress induced as a result of the cooler temperatures during the winter.

Sections 5 and 6, with both five foot and eight foot preformed crack spacing and 0.3 per cent steel, attained the preformed spacing at 201 days and have survived the

TABLE 3.5

CONVENTIONAL CONCRETE AVERAGE CRACK SPACING *

Section No.	7	4	3	1	2	5	6
Preformed Crack Spacing	8	8	5	5	8	5	8
Steel Percentage	0.3	0.4	0.4	0.5	0.5	0.3	0.3
Age of Concrete In Days							
4	8.69	8.00	5.00	5.00	8.00	14.28	8.33
16	8.33	8.00	5.00	5.00	8.00	7.69	8.33
18	8.33	8.00	5.00	5.00	8.00	6.25	8.33
27	8.33	8.00	5.00	5.00	8.00	6.25	8.33
53	8.33	8.00	5.00	5.00	8.00	6.25	8.33
201	8.00	5.40	4.16	5.00	5.40	5.00	8.00
378	6.06	5.00	3.77	4.17	5.00	5.00	8.00

* Measured In Feet

TABLE 3.6

LIGHTWEIGHT CONCRETE AVERAGE CRACK SPACING *

Section No.	10	11	9	8
Preformed Crack Spacing	8'	20'	20'	8'
Steel Percentage	0.3	0.3	0.4	0.4
Age of Concrete In Days				
5	25.00	100.00	200.10	200.00
6	18.18	22.22	200.00	200.00
8	13.33	22.22	200.00	200.00
16	10.00	20.00	100.00	15.38
43	9.52	15.38	15.38	13.33
80	9.09	11.11	12.50	13.33
191	8.69	8.33	9.09	8.00
368	8.00	8.33	9.09	8.00

* Measured In Feet

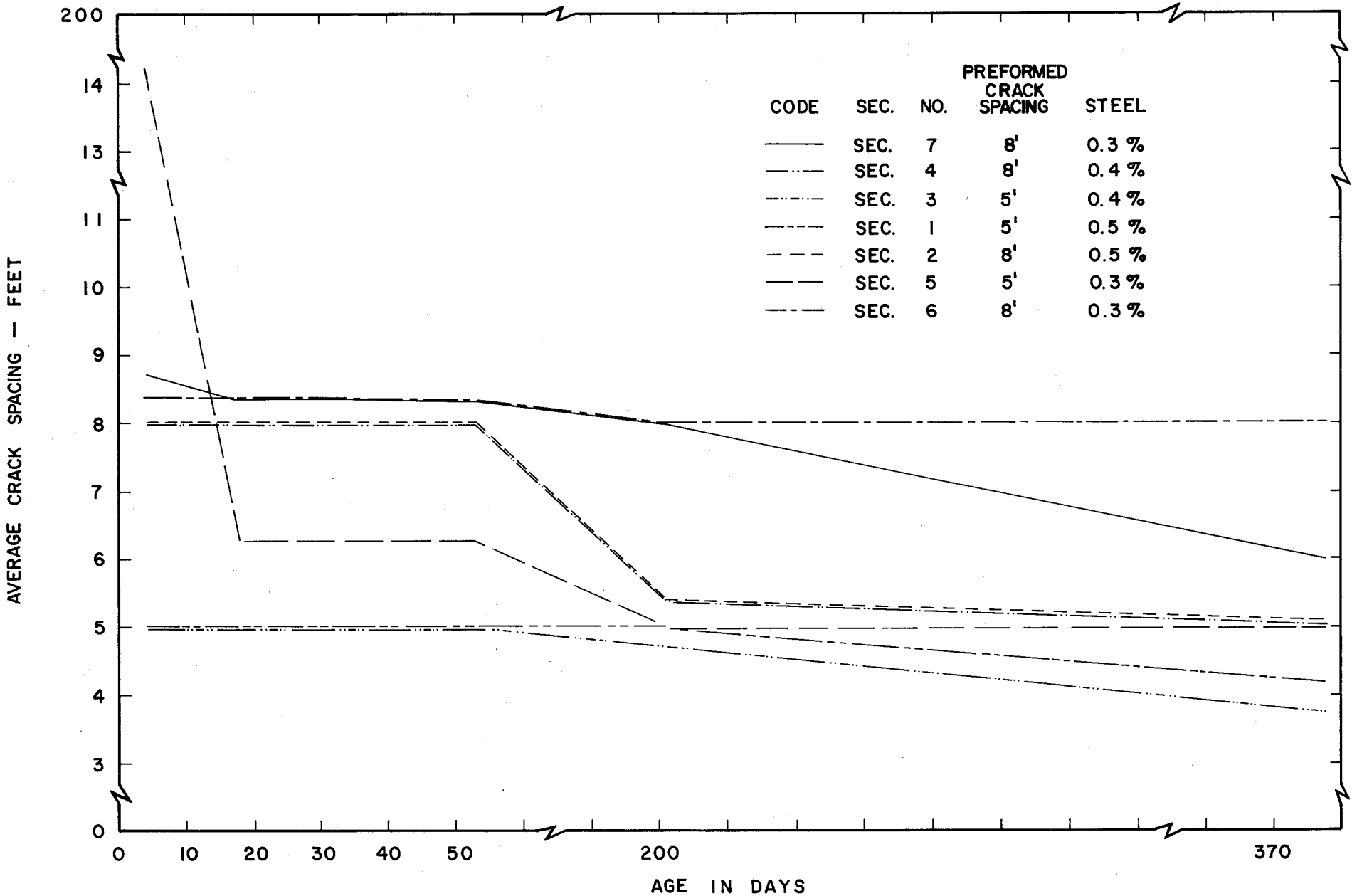

AVERAGE CRACK SPACING VS AGE IN DAYS
CONVENTIONAL CONCRETE

FIGURE 3.1

first maximum stress period (winter) with no additional cracks. Section 7, which also has 0.3 per cent steel and eight foot crack spacing, had cracked almost to the five foot crack spacing. This tends to show that possibly for the conditions of this experiment, that the 0.3 per cent steel with the five foot crack spacing might be the natural combination. The average crack spacing for Sections 1, 3, 4, and 6 with the 0.4 per cent and 0.5 per cent steel, fell below the preformed spacing.

Lightweight CRCP Sections. Figure 3.2 indicates that the lightweight concrete crack pattern was considerably slower in forming than the conventional concrete was. The lightweight sections show little change in the crack spacing between 101 and 368 days. The optimum for both the 0.3 per cent and 0.4 per cent steel sections is approximately eight feet.

Causes of Irregular Crack Patterns. In order to incorporate a regular crack spacing in the steel stress project, volume change cracks were forced to form by use of transverse planes of weakness in the slab. These weakened planes were

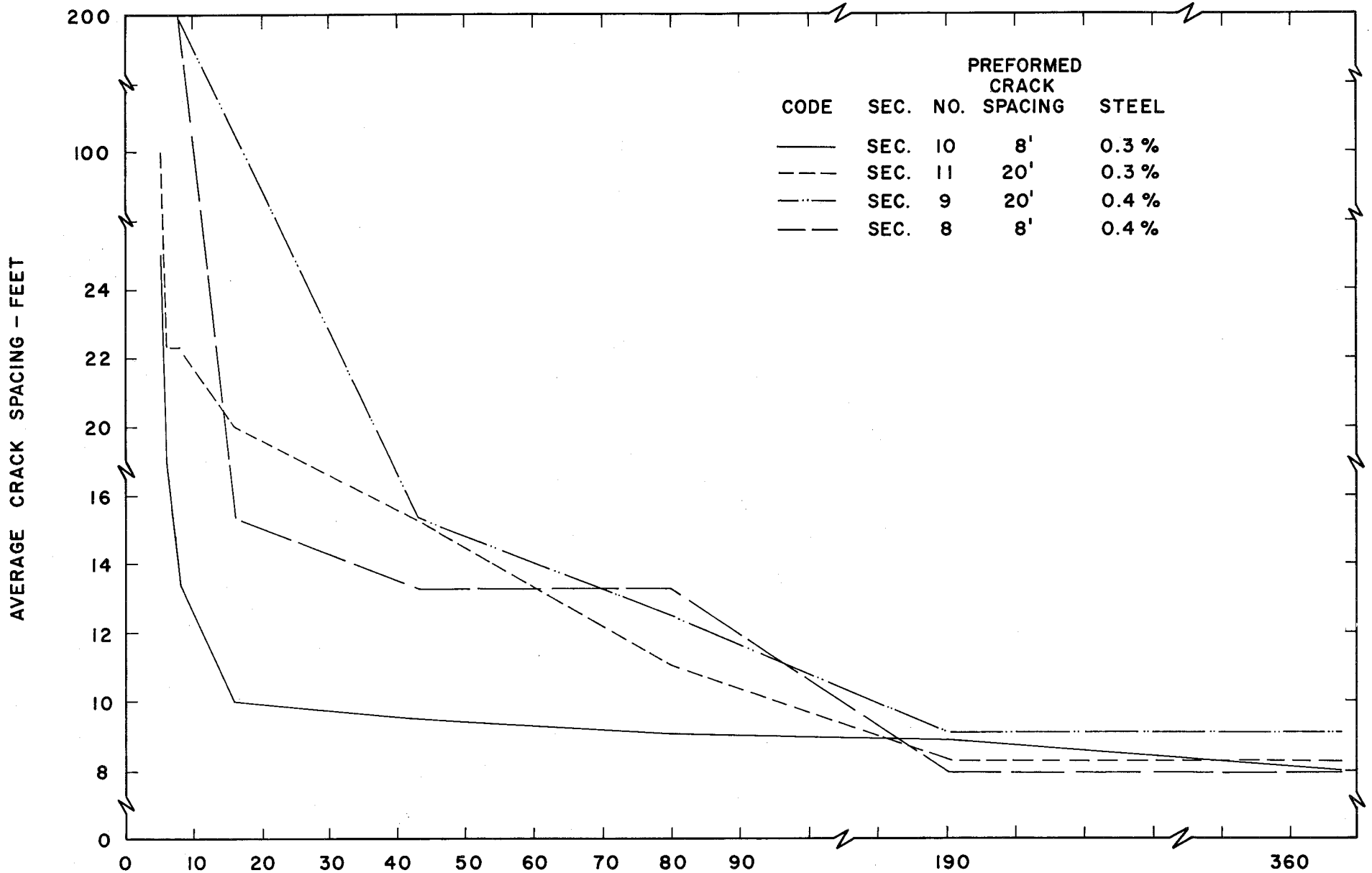

AVERAGE CRACK SPACING VS AGE IN DAYS
LIGHTWEIGHT CONCRETE

FIGURE 3.2

established by placing a piece of corrugated sheet metal four inches high and extending across the width of the pavement at each point where a crack was desired. Most cracks formed in a reasonably straight pattern at the desired points, but a few cracks deviated from the normal pattern to a considerable extent.

The crack with the greatest deviation from the predicted pattern was selected for coring, Figure 3.3. This crack, located in Test Section 6, had a bow of about 14 inches from the predetermined line of cracking and was somewhat irregular in shape. The first core was taken through the crack at one of the points of greatest deviation, approximately half-way across the 24-foot pavement slab. The core of this crack failed to show any irregularities in that no corrugated metal was found, but none was placed at this point. A second core was taken about eight feet from the right-hand curb at a point where the crack more closely followed its preplanned course. This core contained part of the corrugated metal as expected, but it was not in the vertical position and was out of the alignment.

The second core showed that the corrugated metal strip had separated from the base material and had floated in the concrete on its side during the concrete placement, Figure 3.4

Figure 3.3

Texas Highway Department core drilling rig in operation.

Figure 3.4

Core showing abnormal position of corrugated metal.

Figure 3.5

View from outside curb showing crack pattern and core hole.

The core showed that vibration had been good, as the concrete had bonded well to both the reinforcing steel and the corrugated metal and no cavity was found beneath the corrugated metal. With the corrugated metal strip in its sideways position, it served little purpose in forming a weakened plane and the concrete followed the line of least resistance in its cracking, hence its irregular shape as shown in Figure 3.5.

The failure of the corrugated metal to remain in place in a few instances was probably caused by the fact that the steel was placed first and then the corrugated metal was placed to form the joints. This made it difficult to fasten the holders to the base material. This method had been corrected by the time of the next pour by reversing the sequence of construction and the problem was eliminated.

Instrumentation Failure

Eight days after the pouring of the standard CRCP, it was noted that in taking strain gage readings some drift occurred on the voltmeter, and readings became difficult to obtain. This problem became more severe, thus necessitating an investigation into the causes.

On June 30, 1964, the resistance to ground of the strain gage system was investigated. To check the resistance to ground, a three terminal resistance measuring device, a Biddle Megger, was used. With this instrument

it was possible to isolate the insulation of the system into two parts. The first part was the leakage through the cable insulation to ground. This check revealed that the cable's shield was almost completely shorted through the vinyl jacket to ground. However, the individual wires had polyethlene insulation and indicated good but not perfect insulation resistance. The polyethlene insulation had began to fail slowly, but should be good for a few months. The second part of the system that was isolated was the epoxy waterproofing over the gage, the epoxy gage backing, and the connecting wires in the concrete without the covering of the shield. This second part indicated a very low resistance to ground. The probable explanation is that the epoxy waterproofing had failed.

The erratic drift of the strain measuring system seems to have been due to a corrosion problem. The system was responding to a constantly changing voltage generated by the galvanic action of the gage or copper wire with another metal, most likely the zinc coating on the corrugated steel joint. A voltage was actually measured between the cable and ground. This indicated that moisture was present since moisture is necessary for the action to occur.

The VTVM resistance readings were noted to be higher than those of the Biddle Megger. There was a non-linearity of the insulation resistance to different applied voltages.

As a general rule, this is considered an indication of the moisture present in insulation. Again, it was shown that the waterproofing had failed. The VTVM applies a maximum of 1½ volts to the materials under test. The Megger applies either 500 or 1,000 volts.

Subsequent tests are being performed which to date substantiate the reliability of the strain gage cable. This insulation test is a standard ASTM procedure consisting of submerging a length of wire in water and then putting a voltage through the wire. After seven days of soaking, the cable was checked with 500 volts and the insulation was found to be perfect.

A method to recover the operation of the strain gages was not known. If it were possible to stop the galvanic action, there would still be an unknown shorting resistance across the gages which would cause inaccurate readings. Furthermore, this resistance would change as the moisture present changed.

Therefore, it seems probable that any data taken after the twentieth day may be in error due to the epoxy waterproofing failures.

IV. STEEL STRESS ANALYSIS

The development of a relationship encompassing known variables that affect design decisions is one of the main objectives of this project. This chapter deals with the analysis of steel stress in terms of some of these known variables as suggested by a theoretical model.

Theoretical Steel Stress Model

It was felt that a theoretical model would be a starting point in determining any stress-producing factors from the known variables. A theoretical model was derived from which these factors could be studied before actual analysis began. The derivation of this model is presented in Appendix C. Since it has been found that the greatest steel stress occurs at the crack, this was the condition considered for analysis. The following equation portrays this model:

$$S = A_1 \Delta T + \frac{\alpha_c \Delta T E_c}{P} - \frac{E_c}{\bar{X} P}\left[\frac{A_0 Z}{(1+A_2 P)} + \frac{A_3 \bar{X} \alpha_c \Delta T}{P}\right] - \frac{\bar{X}}{P}\left[\frac{A_0 P Z + A_3 \bar{X} \alpha_c \Delta T (1+A_2 P)}{(1+A_5 P X P)}\right]^N$$

Where:

ΔT = temperature differential between mid-depth temperature at concrete set and at the time, t.

α_c = thermal coefficient of concrete

E = modulus of elasticity of concrete, psi

Z = concrete shrinkage, in/in.

$\overline{X}$ = crack spacing, ft.

P = per cent longitudinal steel.

As can be seen, it is almost impossible to arrange this equation into an order that could be analyzed termwise. However, it is believed that ΔT, $\alpha_c E_c \Delta T$, $E_c Z$ are the most important stress-producing factors, along with some combination of P and $\overline{X}$. Therefore, this analysis was conducted considering these factors.

Analysis of Standard CRCP Data

Of the above mentioned variables, temperature differential is probably the greatest stress producer. To study one variable in terms of stress while holding other variables constant, each day of each section was analyzed separately in terms of temperature. This holds all concrete properties as constant as possible and isolates

each per cent steel and crack spacing with each section.

Data Elimination. As mentioned earlier data taken after the twentieth day of pouring was very unstable due to malfunctioning of the strain gages.

Also, rain on the fourth day made estimation of variables, such as shrinkage modulus and moisture content impossible. A close study of some of the stress, time distribution for gages 1, 2, 5 and 6 has shown that some of the preformed cracks did not appear during the initial stages. Considering these factors for the standard CRCP sections, the data taken of the fourth day after concrete placement and all data taken after the eighth day from eight gages was eliminated. Therefore, the study consisted of seven days, six test sections and 15 strain gages, making a total of 7,050 observations. This data set was tested for extreme values. The extreme values were deleted to form the data set used for all analyses presented in this report.

Stress versus temperature. A statistical analysis was run on the change of stress per degree temperature change. This analysis resulted in a straight line given by:

$$S = A_o + B_o T \quad \ldots\ldots\ldots\ldots\ldots\ldots \quad (1)$$

where S is the steel stress at any given temperature change, ΔT. Therefore, B_o is the change in steel stress per degree temperature change and A_o is the steel stress at 0^o temperature change. This analysis was on strain gages 1, 2, 5 and 6 of each section for each daily cycle, as those were the gages at the crack. Then A_o and B_o could be used as a comparison basis for comparing stress characteristics of one test section with another in terms of the factors already discussed.

Change in Crack Spacing. Since crack spacing for each section was changing periodically, the values of the preformed crack spacings could not be used. Table 4.1 shows the average crack spacing for each section for each daily cycle after placement, The steel stress study includes only data taken in the first eight cycles. The crack spacings shown in Table 4.2 were used so that analysis of the other variables could be carried out while holding crack spacing constant.

AVERAGE CRACK SPACINGS FOR EACH SECTION PER CYCLE

SECT.	1	2	3	4	5	6	7	8	9	10	11
CYCLE											
1	-	-	-	-	-	-	-	-	-	-	-
2	5	8	5	8	16.0	8.4	8.9	200	200	200	200
3	5	8	5	8	15.5	8.4	8.9	200	200	100	150
4	5	8	5	8	14.3	8.4	8.7	200	200	50	125
5	5	8	5	8	13.5	8.4	8.7	200	200	25	100
6	5	8	5	8	13.0	8.4	8.7	200	200	18	22
7	5	8	5	8	12.5	8.4	8.6	200	200	15.5	22
8	5	4	5	8	12.0	8.4	8.6	200	200	13	22
9	5	4	5	8	11.5	8.4	8.5	100	200	13	22
10	5	4	5	8	11.0	8.4	8.5	100	190	13	22
11	5	4	5	8	10.5	8.4	8.4	24	175	12	22
12	5	4	5	8	10.0	8.4	8.4	22	160	12	22
13	5	4	5	8	99.5	8.4	8.4	20	145	11	21
14	5	4	5	8	9.0	8.4	8.4	18	130	11	21
15	5	4	5	8	8.5	8.4	8.4	16	115	10	21
16	5	4	5	8	8.0	8.4	8.3	15.4	100	10	20
17	5	4	5	8	7.5	8.4	8.3	15.0	85	10	20
18	5	4	5	8	7.0	8.4	8.3	15.0	70	10	20
26	5	4	5	8	6.3	8.4	8.3	14.0	20	10	20
27	5	4	5	8	6.3	8.4	8.3	14.0	20	10	19
164	5	4	4.8	5.4	6.3	8.2	8.3	10.0	12.5	9.1	9.0
174	5	4	4.8	5.4	6.3	8.2	8.3	10.0	12.5	9.1	9.0
239	5	4	4.8	5.4	5.0	8.0	8.0	8.0	9.1	8.7	8.3
249	5	4	4.8	5.4	5.0	8.0	8.0	8.0	9.1	8.7	8.3
254	5	4	4.8	5.4	5.0	8.0	8.0	8.0	9.1	8.7	8.3
264	5	4	4.8	5.4	5.0	8.0	8.0	8.0	9.1	8.7	8.3
317	4	4	3.6	5.4	5.0	8.0	5.3	8.0	9.1	8.5	8.3
327	4	4	3.6	4.2	5.0	8.0	5.3	8.0	9.1	8.5	8.3
378	4	4	3.6	4.2	5.0	8.0	5.3	8.0	9.1	8.0	8.3
388	4	4	3.6	4.2	5.0	8.0	5.3	8.0	9.1	8.0	8.3

TABLE 4.1

SECTION	$\bar{X}$ (Ft.)
1	5
2	8
3	5
4	8
5	14
7	8.7

AVERAGE CRACK SPACINGS USED IN ANALYSIS OF STEEL STRESS DATA

Table 4.2

B_o versus $E_c \alpha_c$. Plots of B_o versus $E_c \alpha_c$ are shown in Figures 4.1 through 4.6 revealing that the following relationship exists.

$$B_o = A_1 + A_2 E_c \alpha_c$$

where A_1 and A_2 are constants which change for each section. Therefore, A_1 and A_2 are functions of the different sections. Considering the B_o is really the partial derivative of stress with respect to temperature differential, it may be written in the following form:

$$B_o = \frac{\partial S}{\partial T} = A_1 + A_2 (E_c \alpha_c) \quad . \quad . \quad . \quad . \quad (2)$$

Per Cent Steel and Crack Spacing. Since each section has a different combination of per cent steel

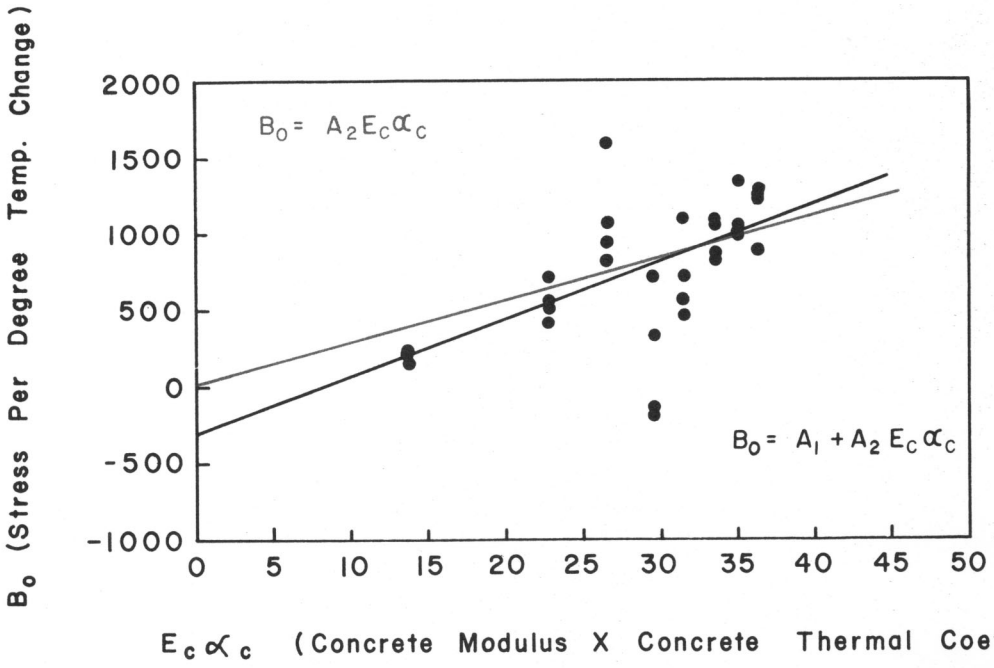

EFFECT OF CONCRETE MODULUS OF ELASTICITY AND THERMAL COEFFICIENT ON STEEL STRESS FOR SECTION I

FIGURE 4.1

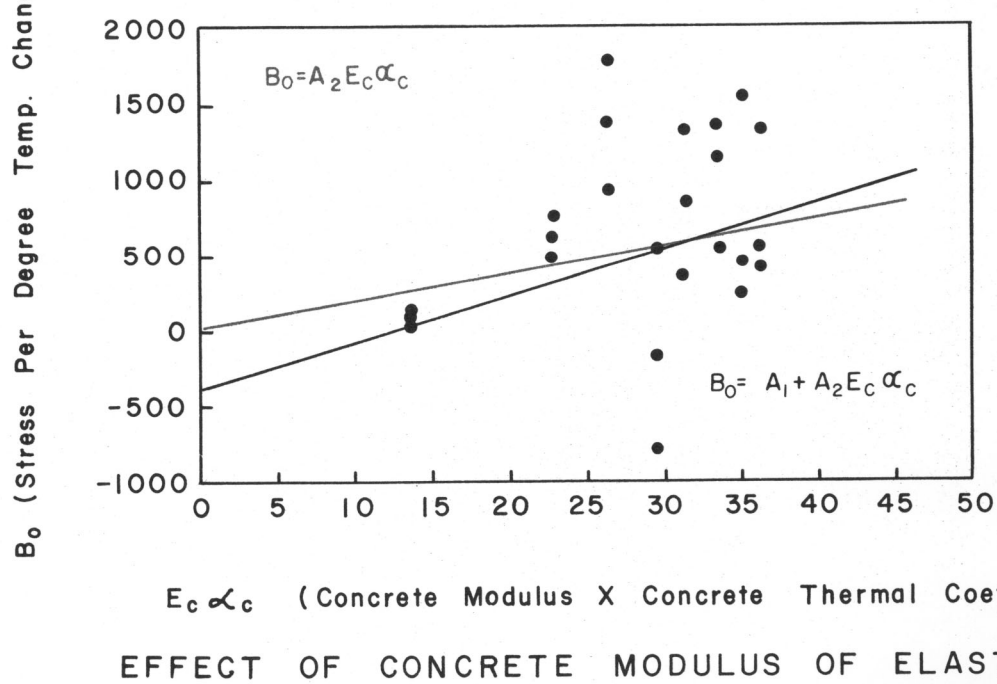

EFFECT OF CONCRETE MODULUS OF ELASTICITY AND THERMAL COEFFICIENT ON STEEL STRESS FOR SECTION 2

FIGURE 4.2

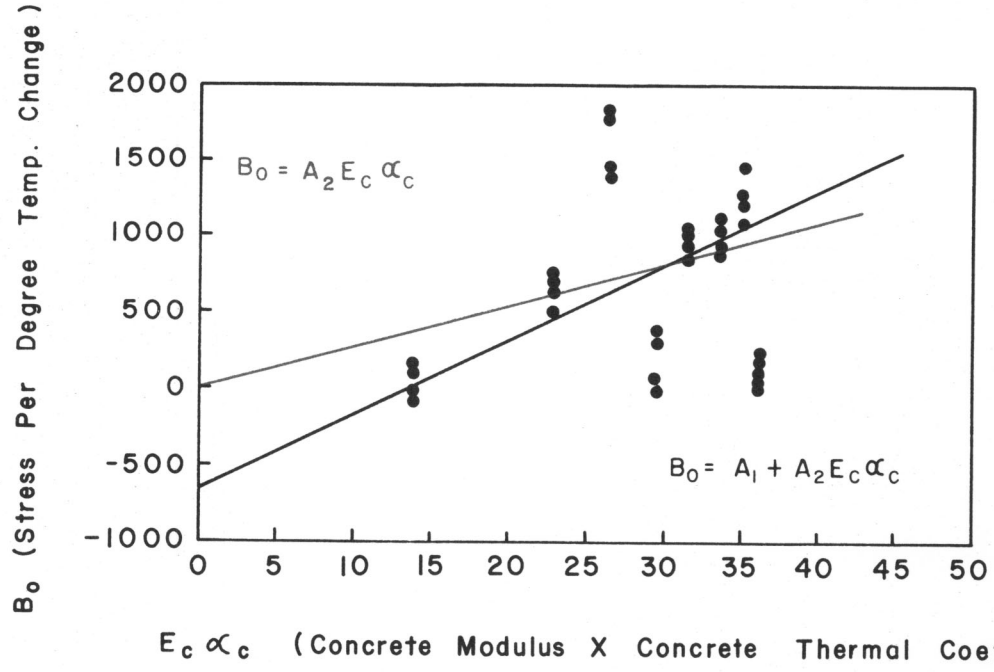

EFFECT OF CONCRETE MODULUS OF ELASTICITY AND THERMAL COEFFICIENT ON STEEL STRESS FOR SECTION 3

FIGURE 4.3

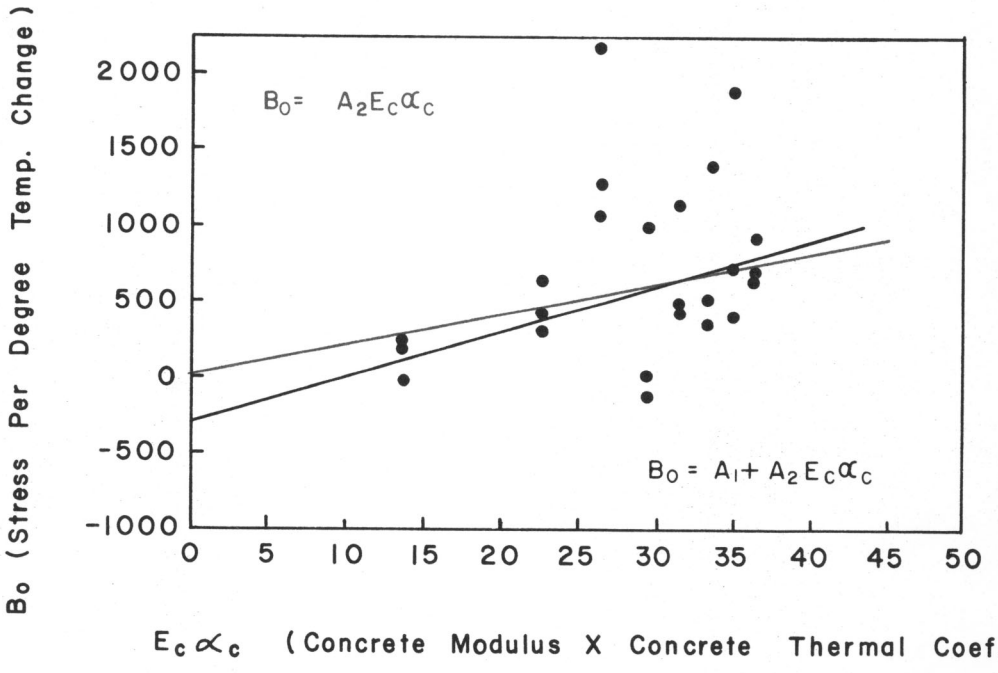

EFFECT OF CONCRETE MODULUS OF ELASTICITY AND THERMAL COEFFICIENT ON STEEL STRESS FOR SECTION 4

FIGURE 4.4

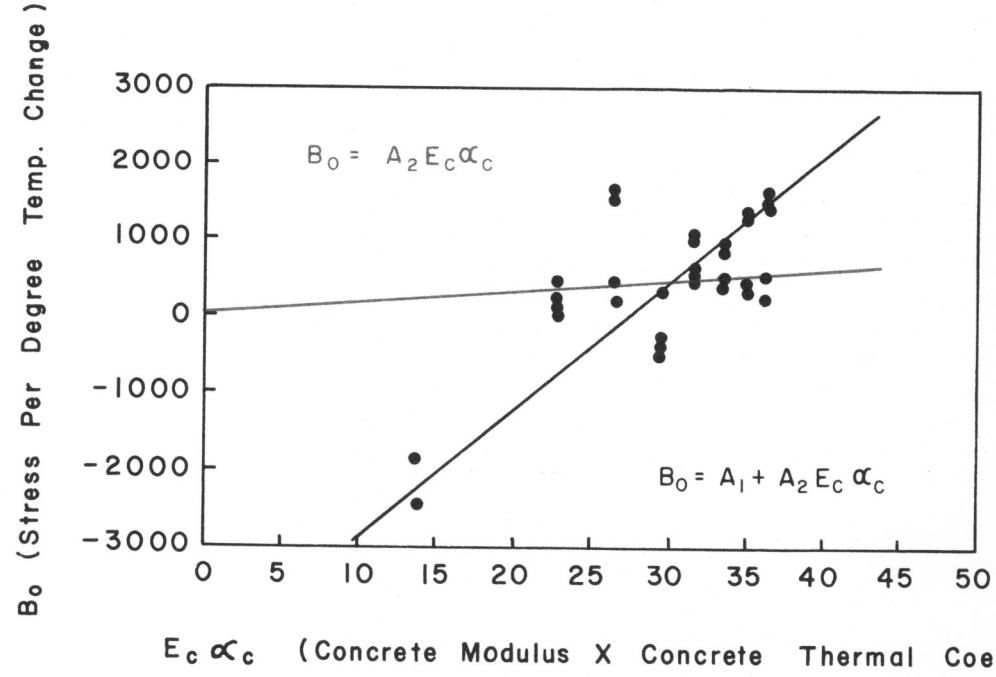

EFFECT OF CONCRETE MODULUS OF ELASTICITY AND THERMAL COEFFICIENT ON STEEL STRESS FOR SECTION 5

FIGURE 4.5

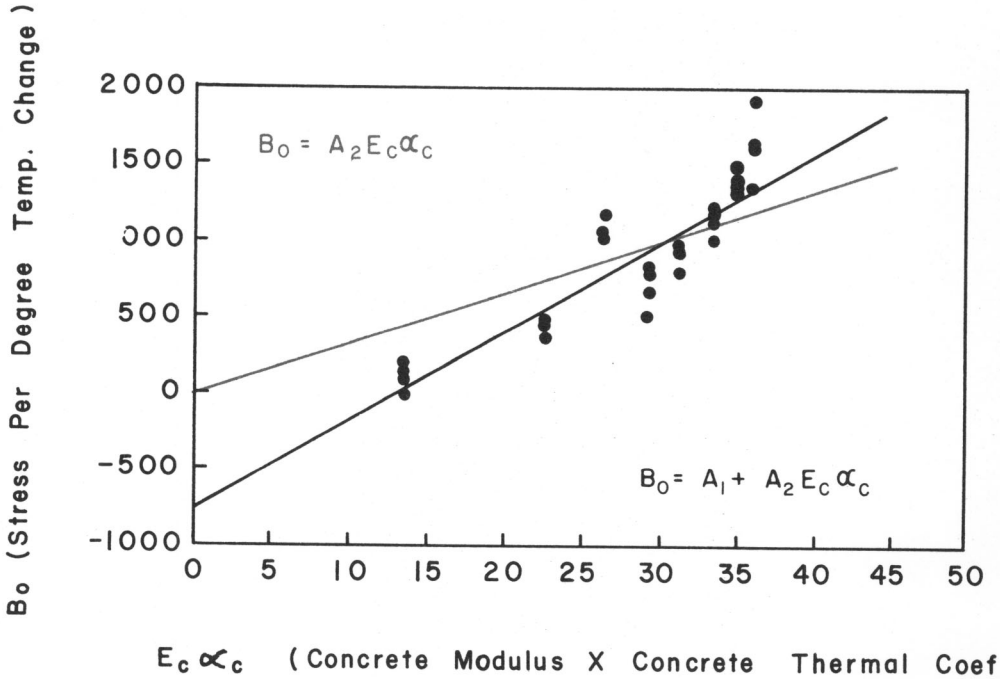

EFFECT OF CONCRETE MODULUS OF ELASTICITY AND THERMAL COEFFICIENT ON STEEL STRESS FOR SECTION 7

FIGURE 4.6

and crack spacing, the A_1 and A_2 terms have to be a function of one of these variables.

Figures 4.7 and 4.8 show A_1 and A_2 plotted versus $\left(\frac{\bar{X}}{P}\right)^2$ for each section. On the basis of these plots, the following relationships for A_1 and A_2 may be stated:

$$A_1 = A_3 + A_4 \left(\frac{\bar{X}}{P}\right)^2 \quad \ldots\ldots\ldots\ldots\ldots (3)$$

$$A_2 = A_5 + A_6 \left(\frac{\bar{X}}{P}\right)^2 \quad \ldots\ldots\ldots\ldots\ldots (4)$$

Substituting Equations (3) and (4) into (2) yields the following:

$$B_o = \frac{\partial S}{\partial \Delta T} = A_3 + A_4 \left(\frac{\bar{X}}{P}\right)^2 + \left[A_5 + A_6 \left(\frac{\bar{X}}{P}\right)^2\right] E_c \alpha_c \quad \ldots (5)$$

To get back ΔT as a variable in this relationship, B_o may be put in integral form as follows:

$$\int_{\Delta T=0}^{\Delta T} B_o \, d\,\Delta T = \int_{S(\Delta T=0)}^{S(\Delta T)} dS$$

Integrating and substituting in for B_o yields:

$$S(\Delta T) - S(\Delta T = 0) = B_o \Delta T$$

$$S(\Delta T) = S(\Delta T = 0) + A_3 \Delta T + A_4 \left(\frac{\bar{X}}{P}\right)^2 \Delta T$$

$$+ \left[A_5 + A_6 \left(\frac{\bar{X}}{P}\right)^2\right] E_c \alpha_c \Delta T \quad \ldots\ldots\ldots (6)$$

RELATION OF PERCENT STEEL AND CRACK SPACING TO STRESS IN STEEL

FIGURE 4.7

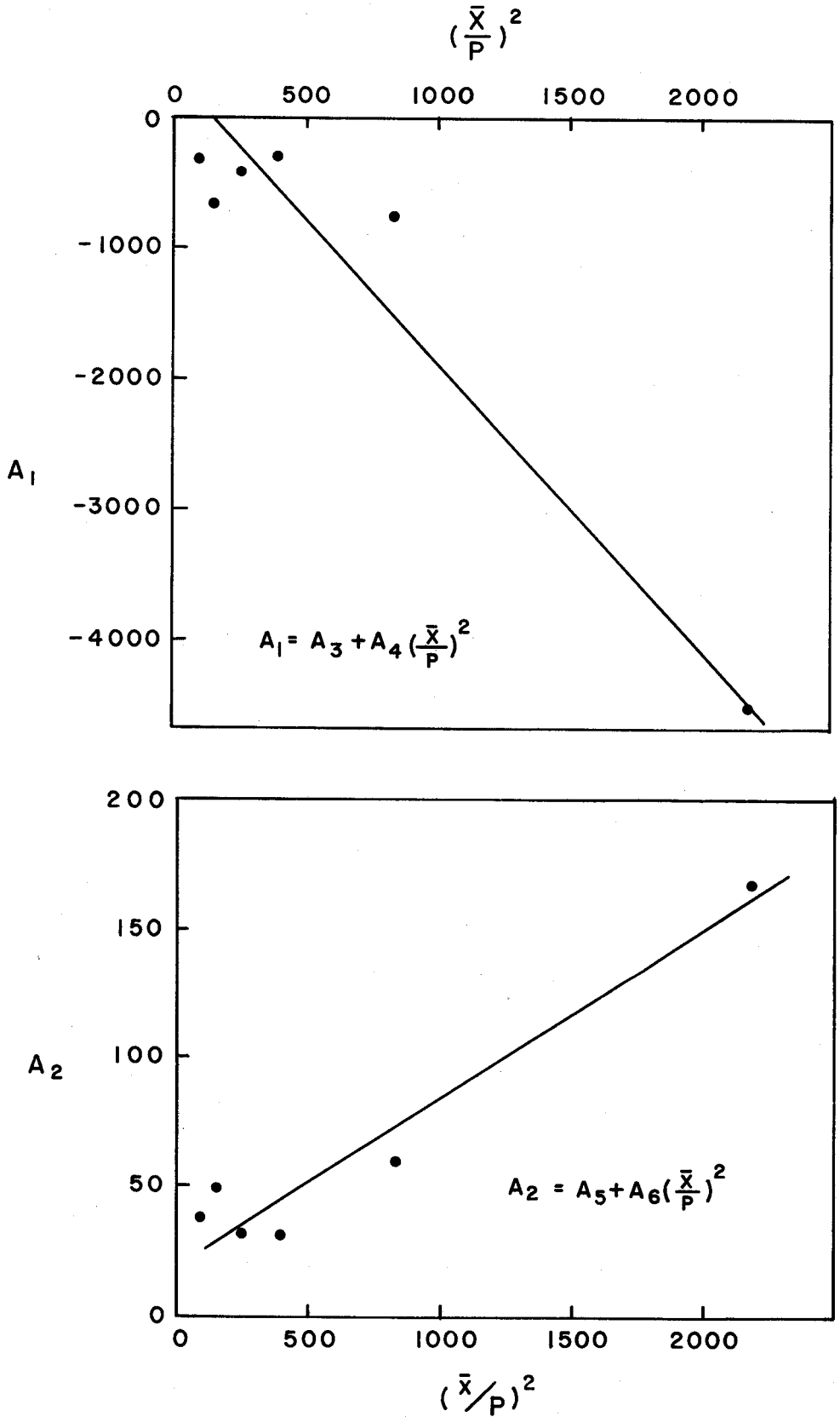

RELATION OF PERCENT STEEL AND CRACK SPACING TO STRESS IN STEEL

FIGURE 4.8

where S (Δ T = 0) = stress at zero temperature change.

A_o versus E_c. It would seem logical that the only stress producers at zero temperature change would be $\overline{X}$, P and the $Z_c E_c$ term. Also, on looking at Equation 1, when $\Delta T = 0$, then $S = f(A_o)$, where A_o is some function of each section. Therefore, the following portrays this functional relationship:

$$S(\Delta T = 0) = f(A_o) = f(\overline{X}, P, Z_c E_c)$$

Figures 4.9 through 4.14 show A_o as a function of $Z_c E_c$ for each section (which hold $\overline{X}$ and P constant). The relationship for these lines are:

$$A_o = A_7 + A_8 (Z_c E_c) \quad . . . . . \quad (7)$$

Here again A_7 and A_8 are different for each section, therefore, they must be some function of $\overline{X}$ and P. Figures 4.15 and 4.16 show the relationships for A_7 and A_8 respectively. The equation format for A_7 and A_8 are given as follows:

$$A_7 = A_9 + A_{10} (\overline{X})^3 \quad . . . . . \quad (8)$$

$$A_8 = A_{11} + A_{12} \left(\frac{1}{P}\right) \quad . . . . . \quad (9)$$

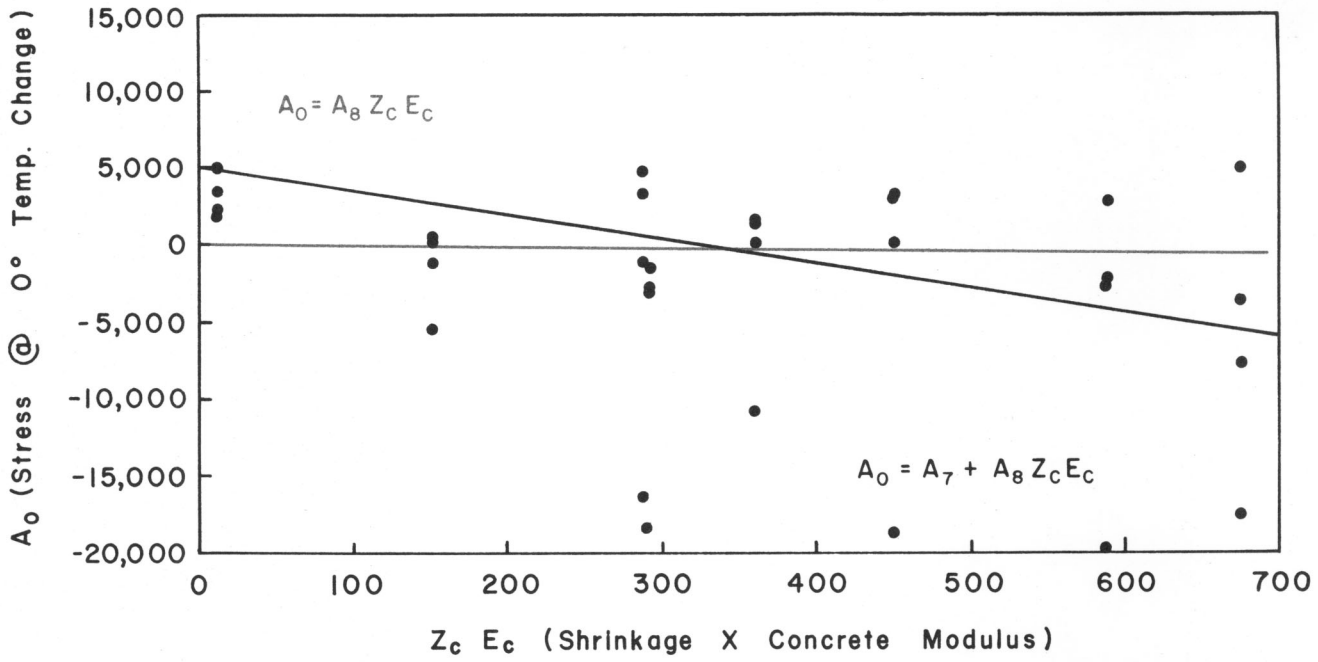

EFFECT OF SHRINKAGE ON STEEL STRESS FOR SECTION I

FIGURE 4.9

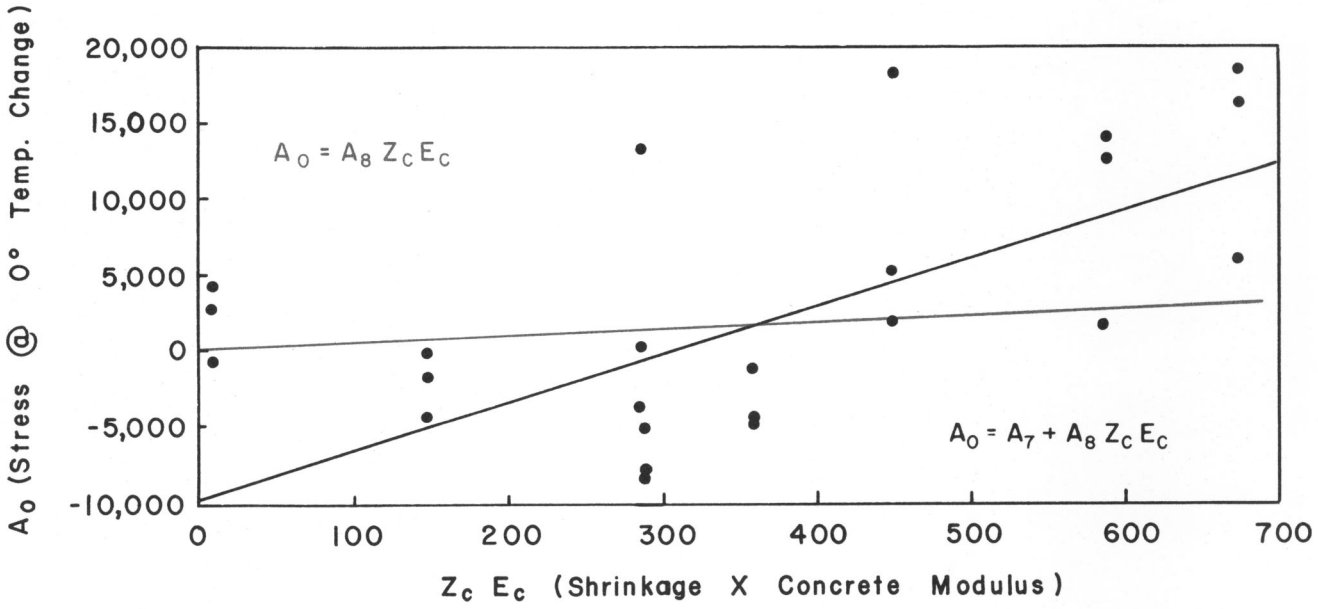

EFFECT OF SHRINKAGE ON STEEL STRESS FOR SECTION 2

FIGURE 4.10

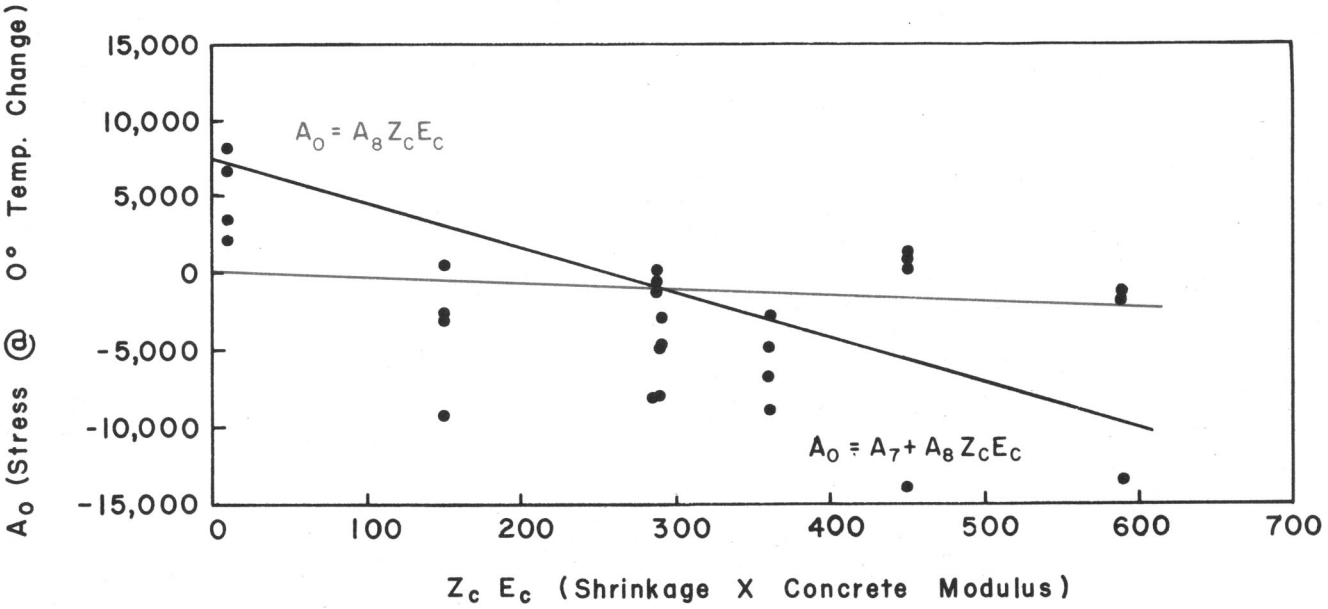

EFFECT OF SHRINKAGE ON STEEL STRESS FOR SECTION 3

FIGURE 4.11

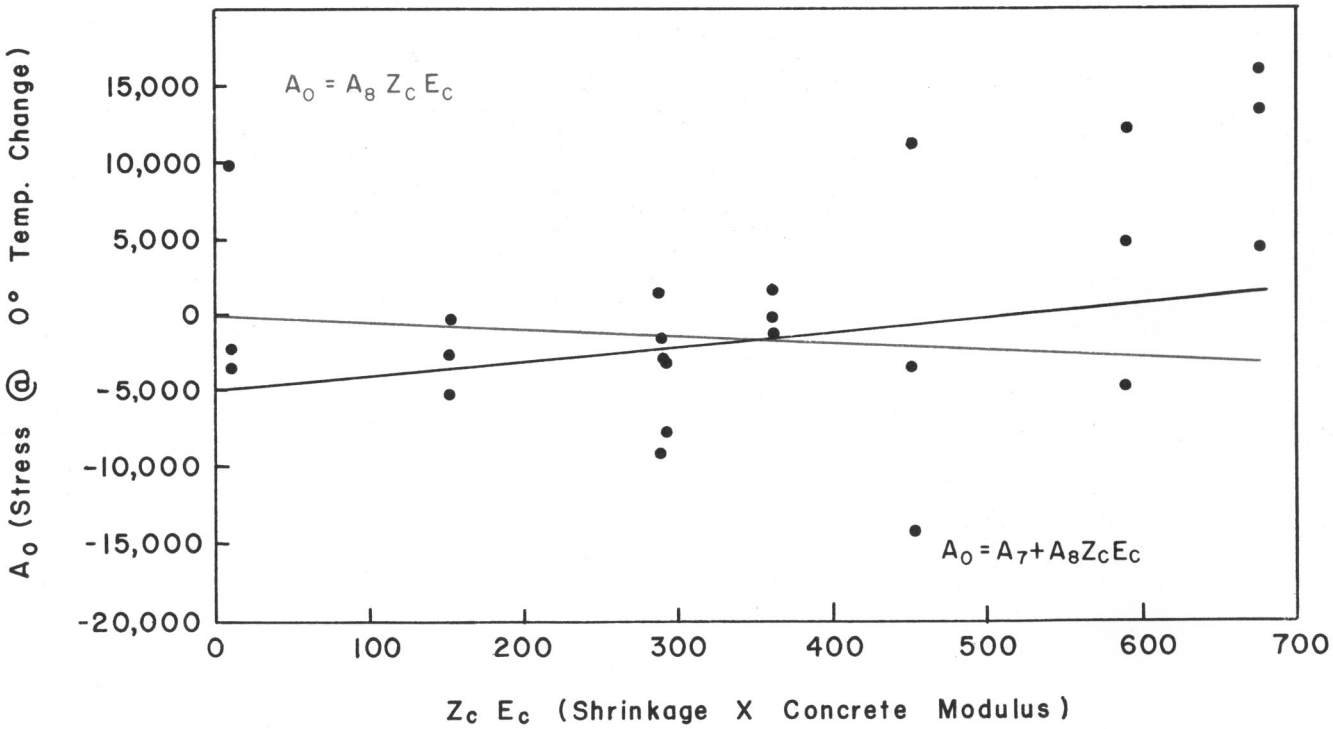

EFFECT OF SHRINKAGE ON STEEL STRESS FOR SECTION 4

FIGURE 4.12

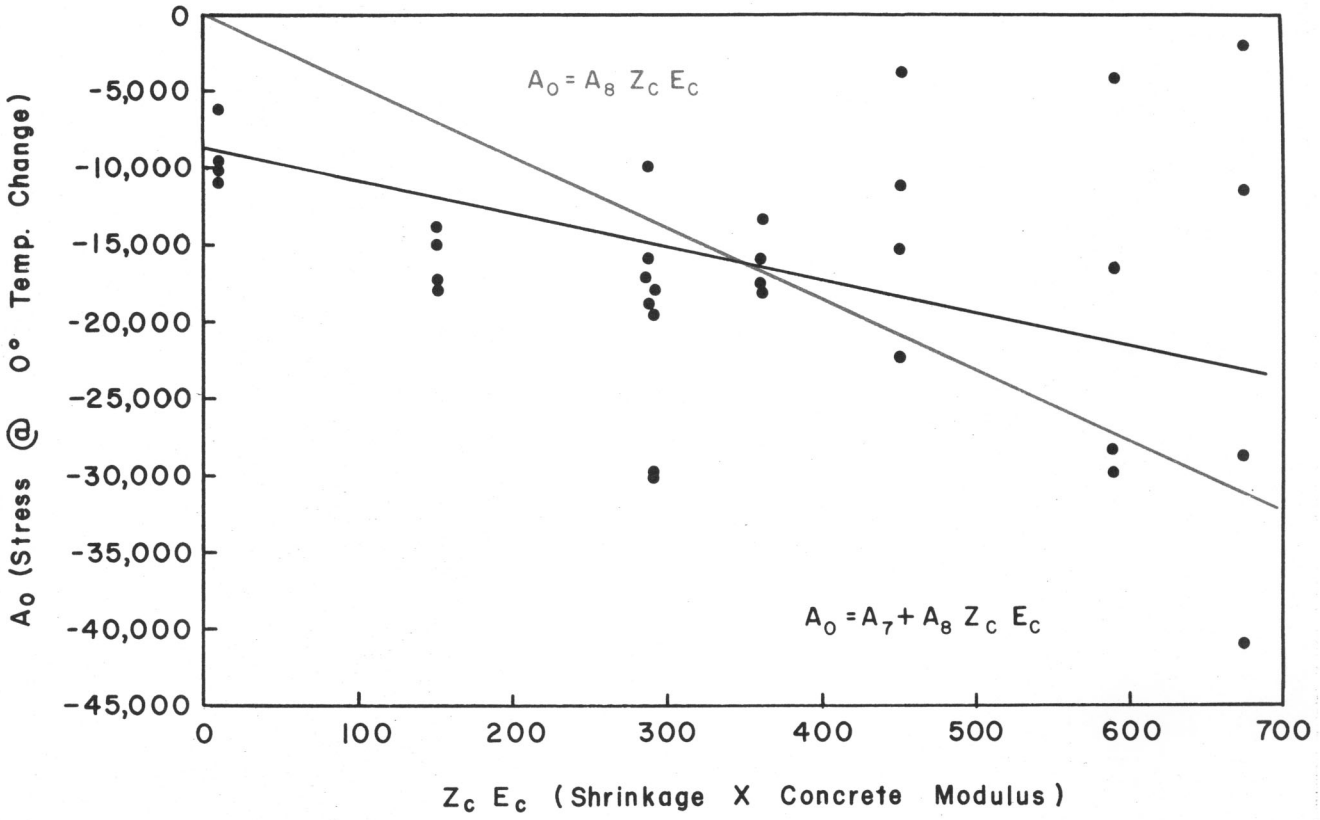

EFFECT OF SHRINKAGE ON STEEL STRESS FOR SECTION 5

FIGURE 4.13

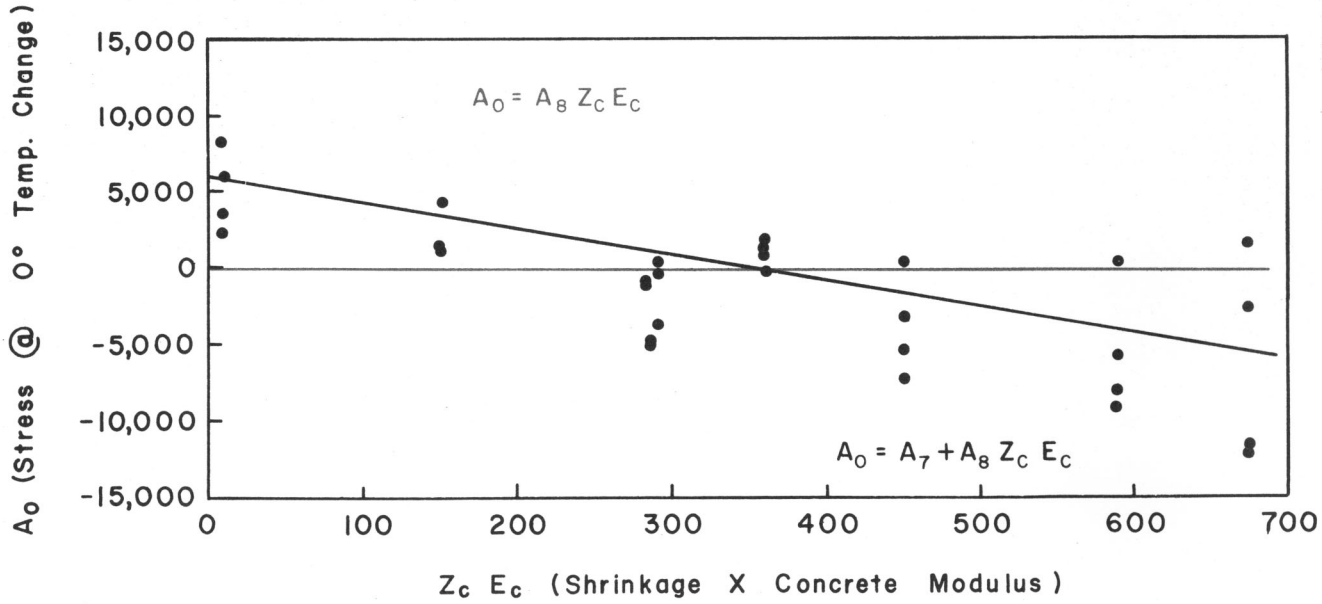

EFFECT OF SHRINKAGE ON STEEL STRESS FOR SECTION 7

FIGURE 4.14

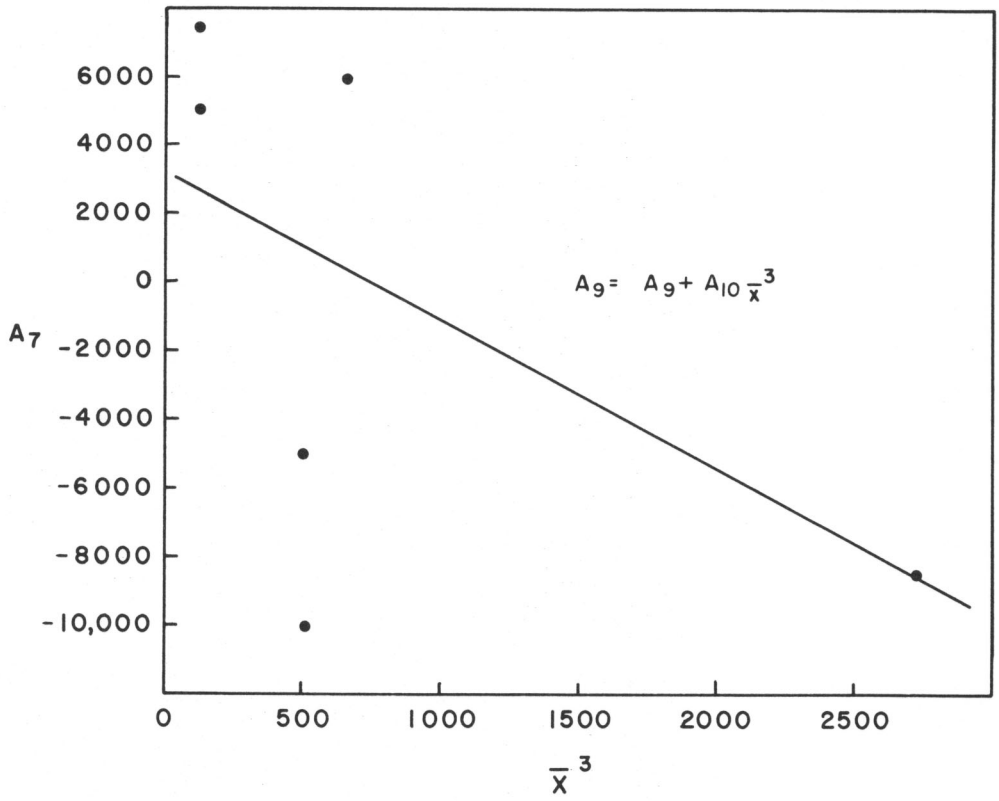

EFFECT OF CRACK SPACING ON STEEL STRESS AT ZERO TEMPERATURE DIFFERENCE

FIGURE 4.15

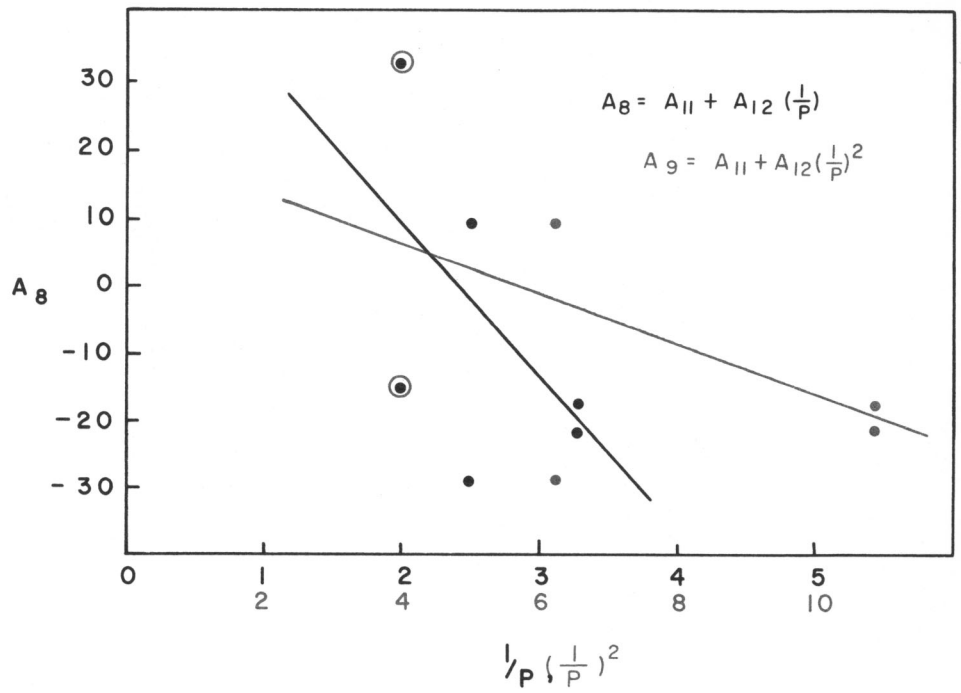

EFFECT OF PERCENT STEEL ON STEEL STRESS AT ZERO TEMPERATURE DIFFERENCE

FIGURE 4.16

Substituting Equations (8) and (9) into (7), yields the following:

$$A_o = A_9 + A_{10}\,(\overline{X})^3 + \left[A_{11} + A_{12}\,\left(\frac{1}{P}\right)\right] Z_c E_c \quad \ldots\ldots \quad (10)$$

It has already been shown however that:

$$S\ (\Delta T = 0) = f(A_o) = f(\overline{X},\ P,\ Z_c\ E_c)$$

Therefore, substituting Equation (10) into (6) and changing subscripts on constants for simplicity yields the following empirical relationship for steel stress in standard CRCP.

$$S = A_1 + A_2\,\overline{X}^3 + Z_c\,E_c\left[A_3 + A_4\,\left(\frac{1}{P}\right)\right] + \Delta T\left\{A_5 + A_6\left(\frac{\overline{X}}{P}\right)^2 + E_c \alpha_c \left[A_7 + A_8\left(\frac{\overline{X}}{P}\right)^2\right]\right\} \quad \ldots\ldots\ldots\ldots \quad (11)$$

First Modification of Empirical Equation

If the equation for stress in the steel should be solved for per cent steel, the solution would be very complex because it exists in quadratic form. Hence it was thought desirable to modify the original model such that the solution for per cent steel would be simpler and more direct.

The modification is shown graphically in Figure 4.16 where A_8 is plotted against $\left(\frac{1}{P}\right)^2$ rather than the $\left(\frac{1}{P}\right)$. The modification is shown in red. This modification greatly simplifies the solution of the stress equation for per cent steel. Now the per cent steel is in squared form in all terms

where it is present. Thus the model for stress in the steel now takes the form

$$S = A_1 + A_2 \bar{X}^3 + Z_c E_c \left[A_3 + A_4 \left(\frac{1}{P}\right)^2\right] + \Delta T \left\{A_5 + A_6 \left(\frac{\bar{X}}{P}\right)^2 + E_c \alpha_c \left[A_7 + A_8 \left(\frac{\bar{X}}{P}\right)^2\right]\right\} \quad (12)$$

Second Modification of Empirical Equation

The second modification of the empirical equation for steel stress is basically another analysis, similar to the first but simpler. The red lines shown in Figures 4.1 through 4.6 and 4.9 through 4.14 graphically show the analysis. The red lines are all drawn through the origin thus eliminating the intercepts which were used for additional analyses in the initial analysis. Following through as in the analysis, Figures 4.1 through 4.6 show for each respective section that $B_o = A_2 E_c \alpha_c$. Next A_2 was correlated to the term $\left[\frac{\bar{X}}{P}\right]^2$ as shown on Figure 4.17.

$$A_2 = A_5 + A_6 \left[\frac{\bar{X}}{P}\right]^2 \quad (13)$$

Also from Figures 4.9 through 4.14 it follows for each section that $A_o = A_8 Z_c E_c$. Next, the A_8 for each section was correlated to $\left[\frac{1}{P}\right]^2$ as shown in Figure 4.18

$$A_8 = A_{11} + A_{12} \left[\frac{1}{P}\right]^2 \quad (14)$$

Now substituting the above values for A_o and B_o into equation (1)

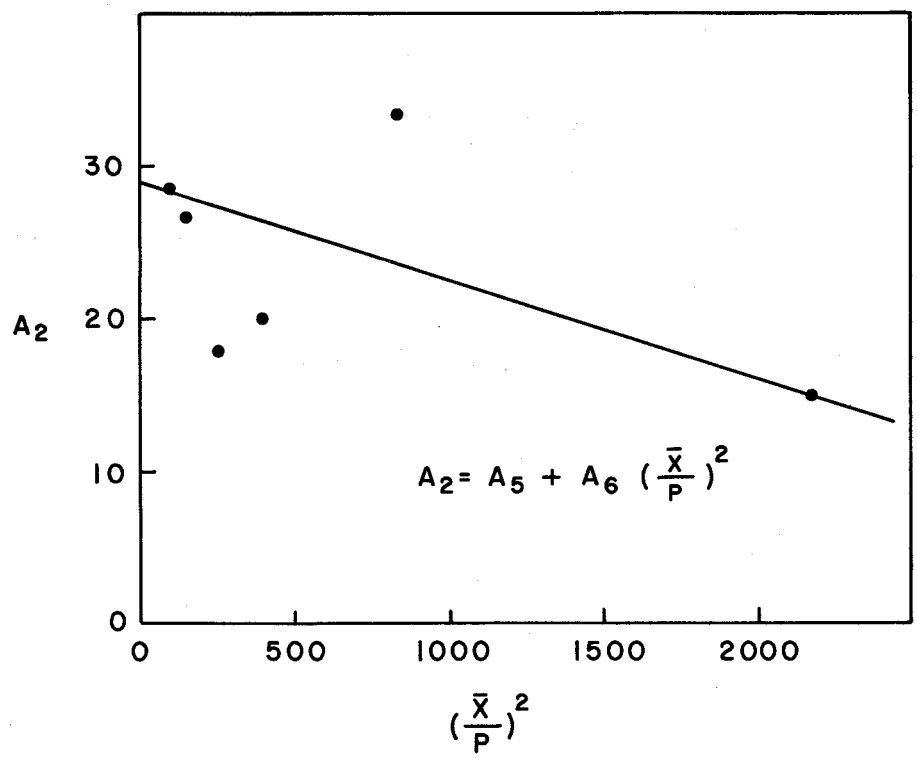

EFFECT OF PERCENT STEEL AND CRACK SPACING ON STRESS IN STEEL

FIGURE 4.17

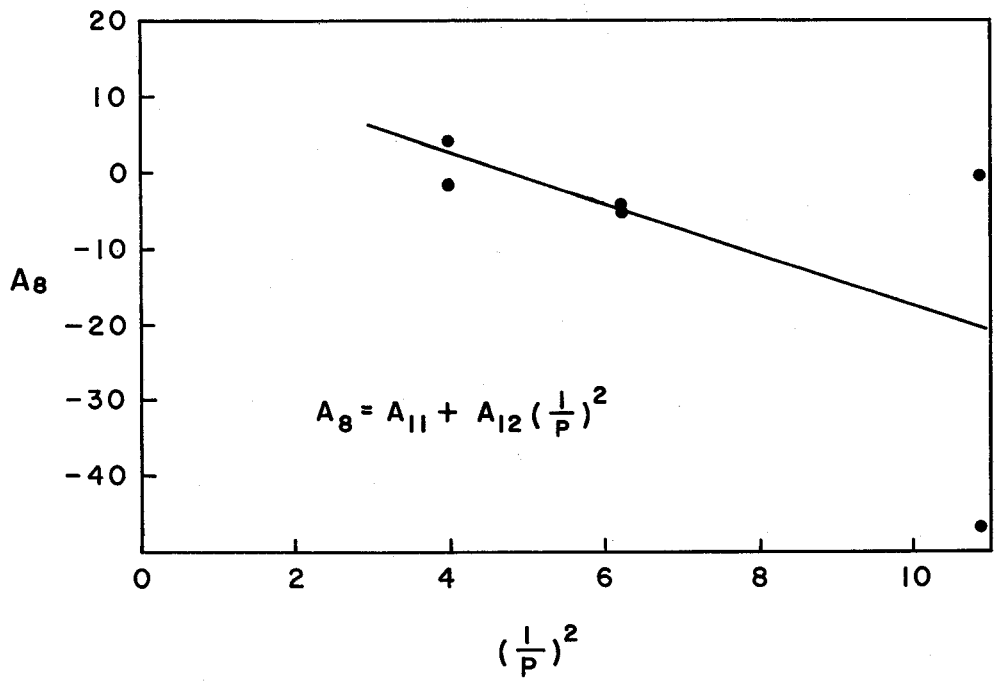

EFFECT OF PERCENT STEEL ON STRESS

FIGURE 4.18

$$S = A_8 Z_c E_c + A_2 E_c \alpha_c \Delta T \quad \ldots\ldots\ldots\ldots\ldots (15)$$

Also substituting (13) and (14) into (15)

$$S = \left\{A_{11} + A_{12} \left[\frac{1}{P}\right]^2\right\} Z_c E_c + \left\{A_5 + A_6 \left[\frac{\bar{X}}{P}\right]^2\right\} E_c \alpha_c \Delta T \quad \ldots (16)$$

Thus, this analysis is a simplified version of the first basic analysis.

Rewriting Equation 17 and changing the constants, the model for stress in the steel now takes the form

$$S = A_1 + A_2 E_c Z_c + A_3 E_c Z_c \left[\frac{1}{P}\right]^2 + A_4 E_c \alpha_c \Delta T + A_5 E_c \alpha \Delta T \left[\frac{\bar{X}}{P}\right]^2 \quad \ldots\ldots\ldots\ldots\ldots (17)$$

Where the constants A_1 through A_5 are determined by regression analysis.

Analysis of Lightweight CRCP Data

Analysis of the lightweight CRCP data was carried out in the same manner as that of the standard CRCP. It should be noted that the standard CRCP sections cracked on the first day while the lightweight sections cracked at a much later time. Also, since the gages began to malfunction shortly after the lightweight sections cracked, insufficient

data was obtained to make any comparison of stresses in the lightweight and standard CRCP. The same general relationships were found to be true in each pavement type, but magnitudes were not comparable.

Evaluation of Empirical Equation for Steel Stress in Standard CRCP

To evaluate Equation 11, a multiple correlation was run using the format of Equation 11 and all of the constants were determined, along with the standard error of estimate and coefficient of determination. The same was done for equations 12 and 17. Listed below in Table 4.3 are their constants.

Regression Constants			Computed Values		
Equation 11	Equation 12	Equation 13	Equation 11	Equation 12	Equation 17
A_1	A_1	A_1	531.478	578.710	3387.126
A_2	A_2		4.093	4.026	
A_3	A_3	A_2	-10.822	-6.475	-18.220
A_4	A_4	A_3	3.666	0.735	2.464
A_5	A_5		-337.930	-333.461	
A_6	A_6		0.498	0.488	
A_7	A_7	A_4	-17.255	-17.388	-27.788
A_8	A_8	A_5	-0.015	-0.014	-0.002
Coefficient of Correlation			0.791	0.792	0.758
Standard Error of Estimate			6913	6909	7378

COMPUTED CONSTANTS FOR EMPIRICAL EQUATIONS

TABLE 4.3

Table 4.4 compares stresses computed from the three models evaluated. The positive values are tensile stresses and negative are compressive as was the notation on the data from which the equations were developed. Also, note that ΔT may be represented as follows:

$$\Delta T = (T_n - T_o)$$

where:

T_n = pavement temperature at any time

T_o = pavement temperature at time of concrete placement

Since this equation is of empirical nature and derived using observed data, care should be taken in using data only in the range of this experiment. Table 4.5 shows maximum and minimum values that should not be exceeded when using this equation.

VARIABLE	MAXIMUM VALUE	MINIMUM VALUE
$\overline{X}$	14 Ft.	3 Ft.
P	0.5%	0.3%
Z_c	118×10^{-6}	3×10^{-6}
E_c	5.72×10^{6}	3.12×10^{6}
α_c	6.34×10^{-6}	4.40×10^{-6}

LIMITS OF VARIABLES FOR USE IN STEEL STRESS EQUATION

Table 4.5

AVERAGE CRACK SPACING	PERCENT STEEL	SHRINKAGE x TEMPERATURE CHANGE	CONCRETE MODULUS x THERMAL COEFFICIENT											
		CONCRETE MODULUS	30						36					
			300			900			300			900		
			-30	-10	10	-30	-10	10	-30	-10	10	-30	-10	10
5	0.3		26700	9900	-7000	27600	10700	-6100	30600	11200	-8200	31400	12000	-7400
			26700	10000	-6800	27700	11000	-5800	30500	11200	-8000	31500	12200	-7000
			31700	14600	-2400	37100	20100	3100	36800	16300	-4100	42200	21800	1400
	0.4		26000	9000	-7900	25000	3000	-8900	29500	10200	-9100	28500	9200	-10100
			25900	9000	-7900	24700	7800	-9000	29400	10100	-9100	28200	9000	-10200
			27800	11000	-5900	26100	9300	-7600	32900	12700	-7600	31200	10900	-9300
	0.5		25500	8500	-8500	23400	6400	-10600	28900	9600	-9600	26800	7500	-11700
			25500	8500	-8500	23400	6400	-10600	28900	9600	-9600	26700	7500	-11700
			26100	9300	-7500	21000	4200	-12600	31100	11000	-9200	26100	5900	-14200
8	0.3		27700	11300	-5200	28500	12100	-4300	32700	12900	-6800	33600	13800	-6000
			27400	11200	-4900	28400	12200	-3900	32300	12900	-6600	33300	13900	-5500
			32500	14900	-2700	37900	20400	2800	37700	16700	-4400	43200	22100	1000
	0.4		27200	10500	-6200	26200	9500	-7200	31400	11900	-7600	30400	10900	-8600
			26900	10400	-6200	28500	9200	-7300	31100	11700	-7600	29900	10600	-8700
			28300	11100	-6100	26600	9400	-7800	33500	12800	-7800	31700	11100	-9500
	0.5		26900	10000	-6800	24800	7900	-8900	30700	11300	-8100	28600	9200	-10200
			26700	10000	-6800	24600	7800	-8900	30500	11200	-8100	28400	9100	-10200
			26400	9400	-7600	21300	4300	-12700	31500	11100	-9300	26400	6000	-14400

PREDICTED STRESSES USING EMPIRICAL EQUATIONS

* First Analysis
* First Modification
* Second Modification

TABLE 4.4

V. CONCRETE MOVEMENT ANALYSIS

The volume change cracks in continuously reinforced concrete pavement appear mysterious to many highway engineers. These cracks and their widths are quite important and many times are not given much thought. This chapter contains an analysis of these crack widths in terms of some of the known variables which are suggested in the following theoretical model.

Theoretical Crack Width Model

In order to properly analyze variables that effect crack width, a theoretical crack width model for concrete movement was developed. The derivation of this theoretical concrete movement or crack width model is presented in Appendix D. The following equation portrays this model.

$$Dx = \frac{A_0 \, d/4r}{1 + A_2 P + \frac{A_3 P}{S'_c}} \cdot Z + \frac{A_4 \bar{X} \alpha (t_0 - t_n)}{(K+1)(P+1)}$$

Where: Dx = crack width

d = bar diameter

r = coefficient of bond properties

P = steel area to concrete area ratio

U = Effective bond stress, psi.

$S'c$ = Tensile strength of concrete, psi.

Z = Shrinkage coefficient of concrete

$\overline{X}$ = Crack spacing, ft.

α_c = Thermal coefficient of the concrete, ^{o}F.

t_o = Reference temperature, ^{o}F.

t_n = Temperature at any time, ^{o}F.

K = Subbase coefficient of friction

A_o, A_2, A_3, A_4 - Unknown constants

As can be seen in the theoretical model, crack width is caused by two main factors. These being: shrinkage and temperature. This theoretical model was used as a basis in analyzing the data which is presented in the rest of this chapter. Only the data from the standard CRCP was analyzed, because the crack pattern did not develop as intended on the lightweight concrete.

Analysis of Data

Movement data was taken on all the gages between the cracks as well as the gages across the cracks. This was done in order to establish whether or not the entire slab lengths between cracks were contributing to the crack widths.

A linear regression was run on the data taken each day on each gage. The regression related concrete movement to temperature change. The temperature change might be defined as the concrete slab temperature at placement less the slab temperature at the time when making a measurement. The form:

$$Dx = C_o + D_o \Delta T \quad \ldots\ldots\ldots\ldots\ldots\ldots \quad (3)$$

Where:

Dx = Concrete movement, in.

ΔT = Slab temperature change, ^{o} F.

C_o and D_o are regression constants

To determine if the entire slab segment between two cracks was experiencing movement, the D_o term from the linear regressions was plotted against the distance from the crack which can be represented by the gage number. An example of this type of graph is shown in Figure 5.1. This graph indicates that the entire slab length or that the actual crack spacing is the effective crack spacing. The effective crack spacing is the length of slab between transverse cracks that contributes to the width of the cracks.

As concrete ages the coefficient of thermal expansion changes. This change in thermal coefficient was related to concrete movement by plotting the movement represented

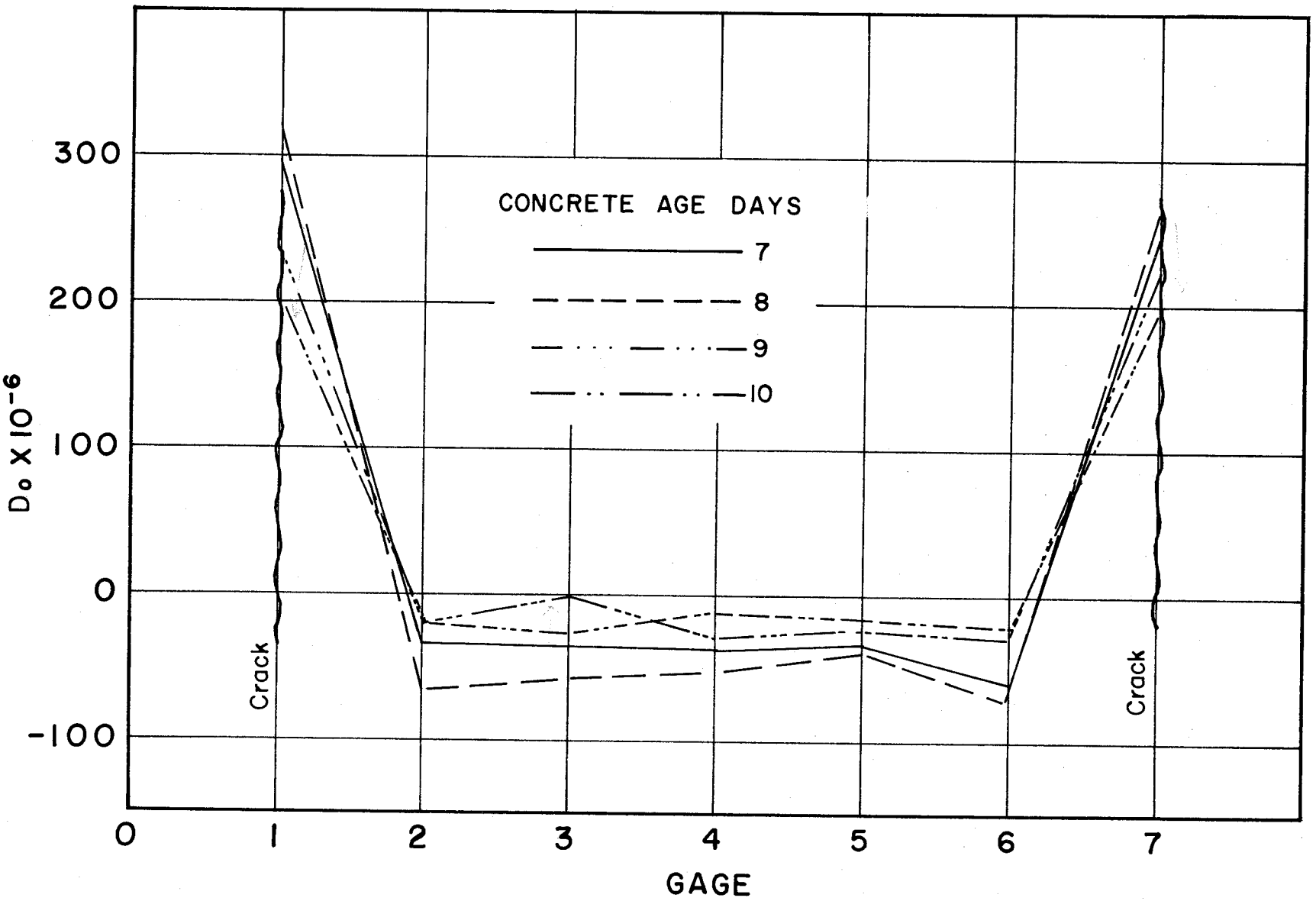

MOVEMENT ALONG SLAB SEGMENT

FIGURE 5.1

by A_o term against the coefficient of thermal expansion of the concrete. A typical graph of this type is shown in Figure 5.2. It appears that the slight change in coefficient of thermal expansion does have some effect on the movement as is shown graphically in Figure 5.2.

The shrinkage of the concrete which is theoretically one of the two reasons for cracks in concrete was found to affect movement linearly. Figure 5.3 is a typical graph of shrinkage versus movement. The shrinkage properties of the concrete changed with the weather conditions when the concrete was less than 20 days old. The shrinkage was increased significantly during periods of wet weather.

The above analyses indicate that the concrete crack width is a function of the parameters indicated in the theoretical formula.

Correlation of Parameters

The crack widths or movement of the concrete at a crack was analyzed to develop an equation for prediction of crack widths. The "classical" engineering formula for calculating movement in a material such as concrete might be written as:

$$CDx = -(\overline{X}\ (Z_i - Z_o) + \overline{X}\alpha c\ (t_o - t_n)) \quad (4)$$

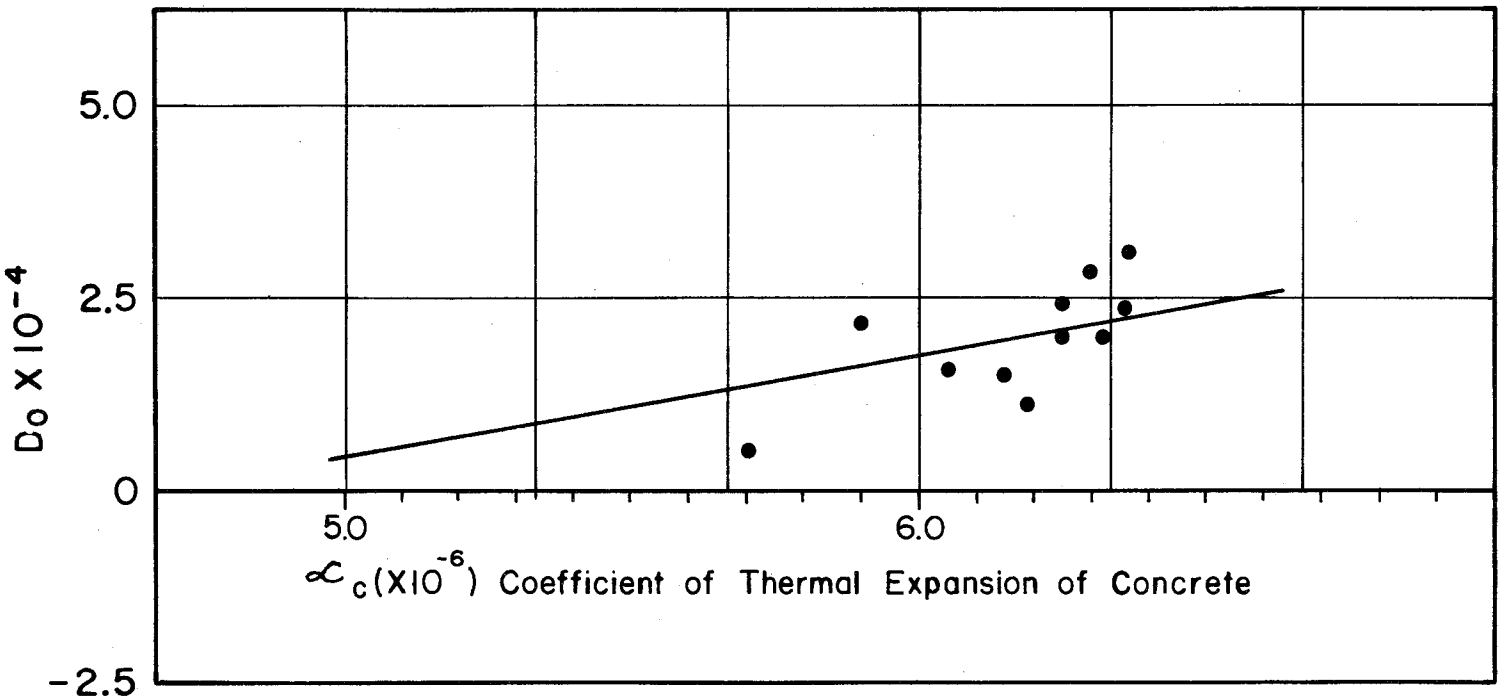

EFFECT OF COEFFICIENT OF THERMAL EXPANSION ON CONCRETE MOVEMENT

FIGURE 5.2

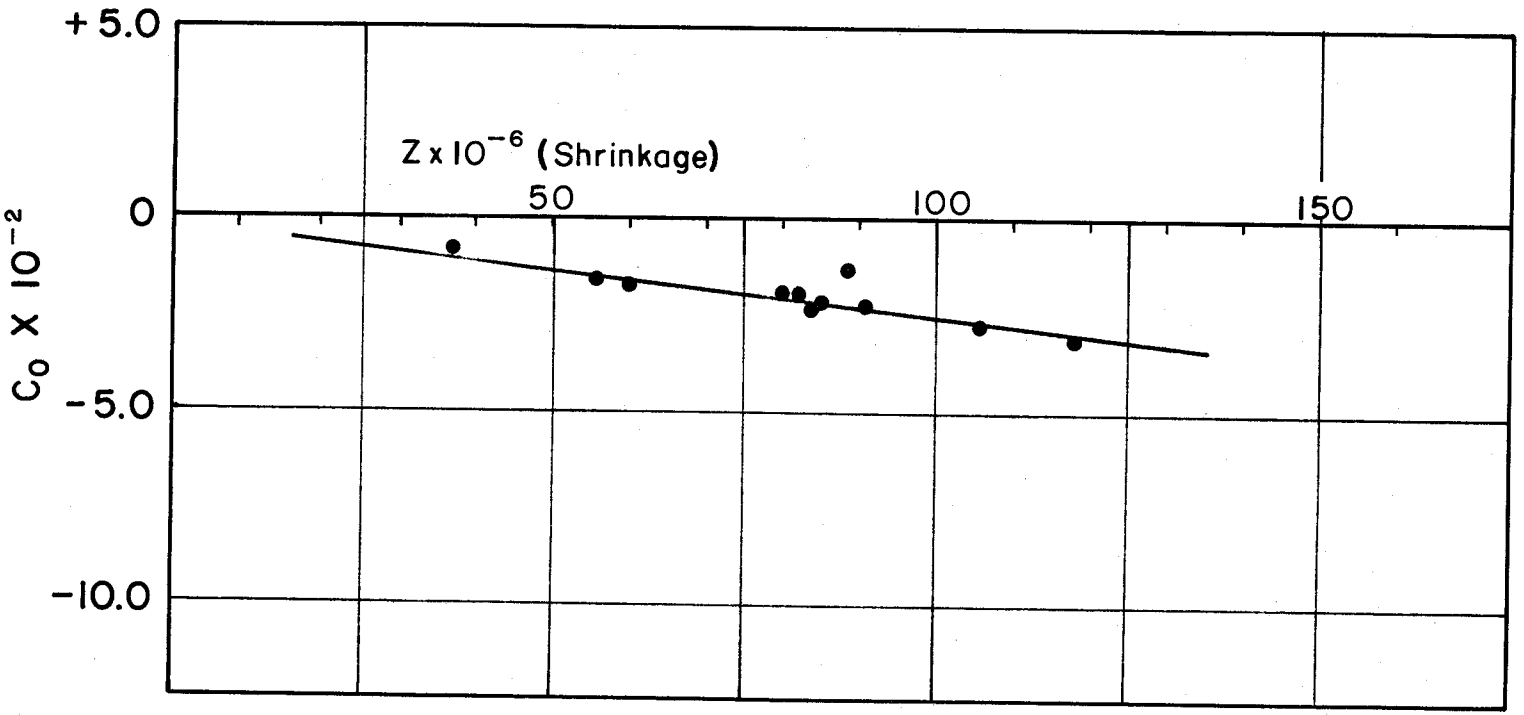

EFFECT OF SHRINKAGE ON CONCRETE MOVEMENT

FIGURE 5.3

$$CDx = -(\overline{X}\ (\Delta Z) + \overline{X}\ \alpha_c\ \Delta T \quad \ldots\ldots\ldots\ldots (5)$$

Where:

CDx = calculated movement, in.

$\overline{X}$ = slab length

Z = change in shrinkage, in/in.

α_c = coefficient of thermal expansion, ^{o}F.

ΔT = change in temperature, ^{o}F.

This "classical" formula is a version of the theoretical formula presented earlier.

To begin this analysis of crack widths or concrete movement at the crack position, the crack width was correlated to temperature on each of six sections on the standard CRCP. A typical graph of this analysis is shown in Figure 5.4. Over the entire range shown, the crack width-temperature relationship is not linear, but curvalinear. A linear regression was made on each of the six sections under study and then the data from all six sections were combined and analyzed.

The graphs of the temperature-crack width relationship were very much the same for all six test sections. Figure 5.5 shows a graph of all the data illustrating the general

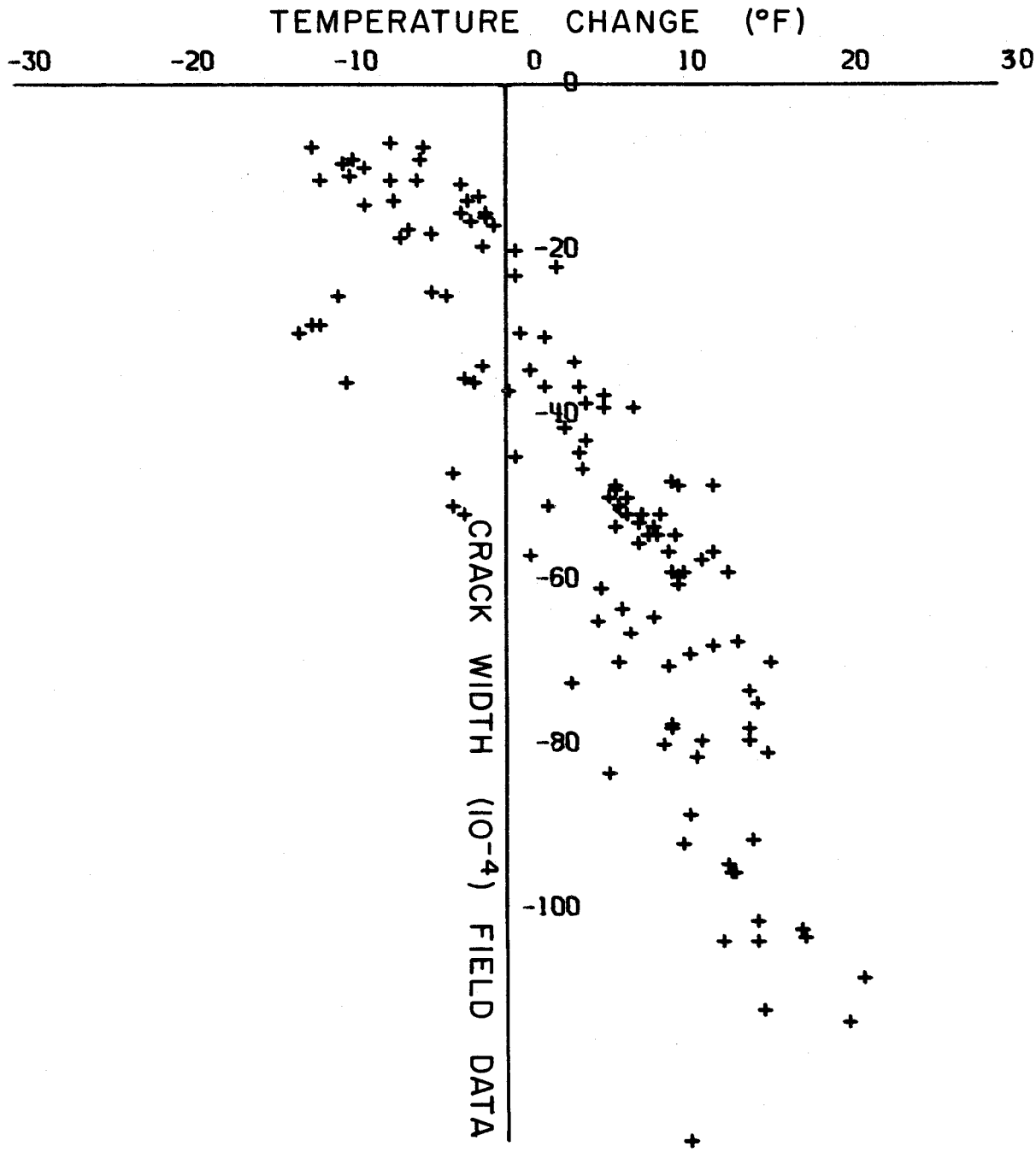

EFFECT OF TEMPERATURE CHANGE ON CRACK WIDTH

Figure 5.4

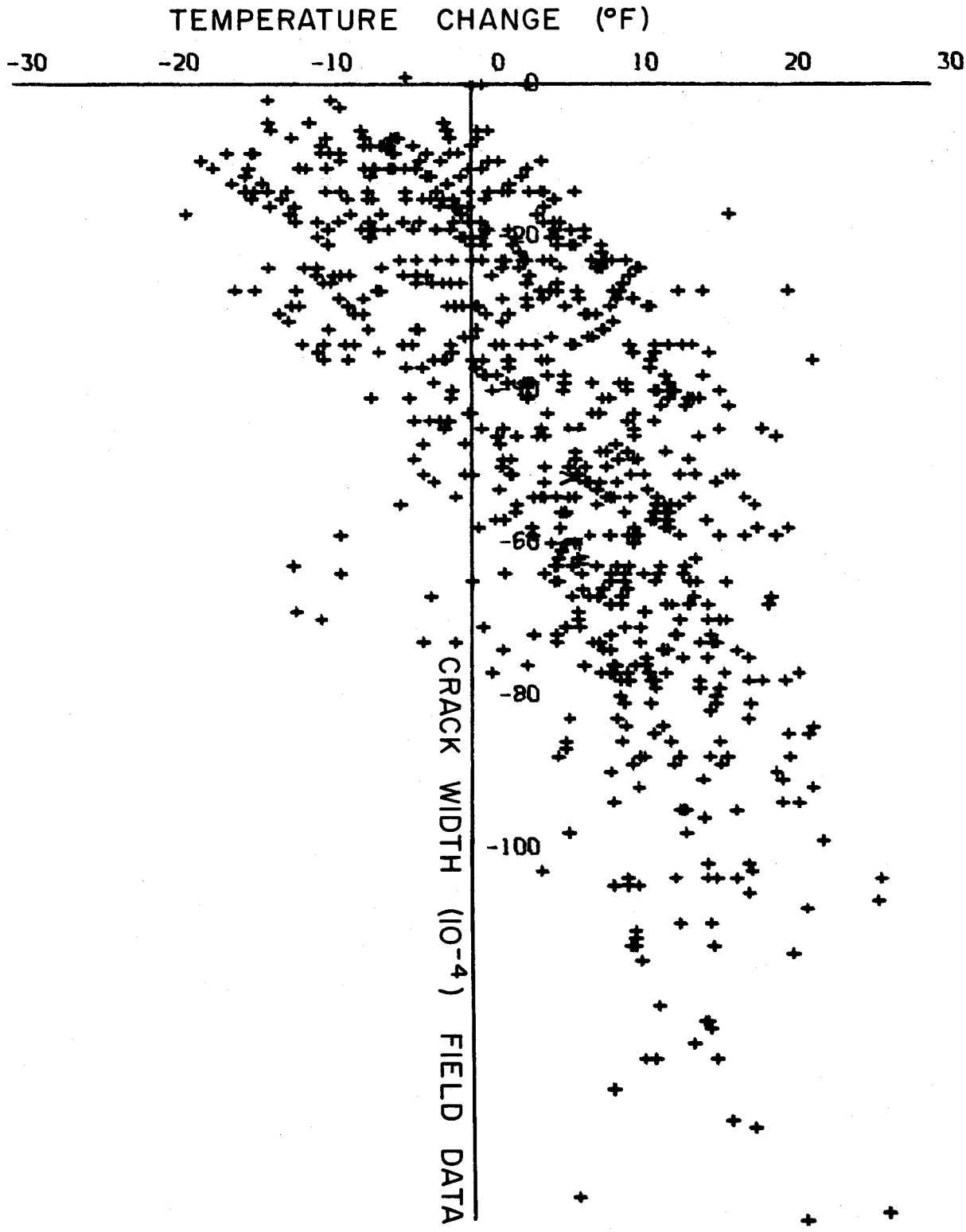

EFFECT OF TEMPERATURE CHANGE ON CRACK WIDTH

Figure 5.5

relationship of crack width to the temperature change associated with each section.

For each field crack width measurement that was made, a corresponding calculation was made using the "classical" formula discussed earlier. These calculated values were studied and compared with the field data to establish any correlation that might exist. The comparisons from each test section indicated some correlation. Figure 5.6 is a typical portrayal of what correlation existed between the data and the calculations by the "classical" formula. Thus, it now becomes evident that some modification of this classical formula might serve as a model equation for predicting crack widths in CRC pavements.

Model Study

The primary differences of the six test sections were crack spacing and per cent longitudinal steel. The crack spacing is in the classical formula, thus leaving the per cent steel as a tie between the sections. The range on per cent steel was from 0.3 to 0.5 per cent which is a quite narrow range. The following equations are four different models which were investigated. Each of these models is a modification of the "classical" formula:

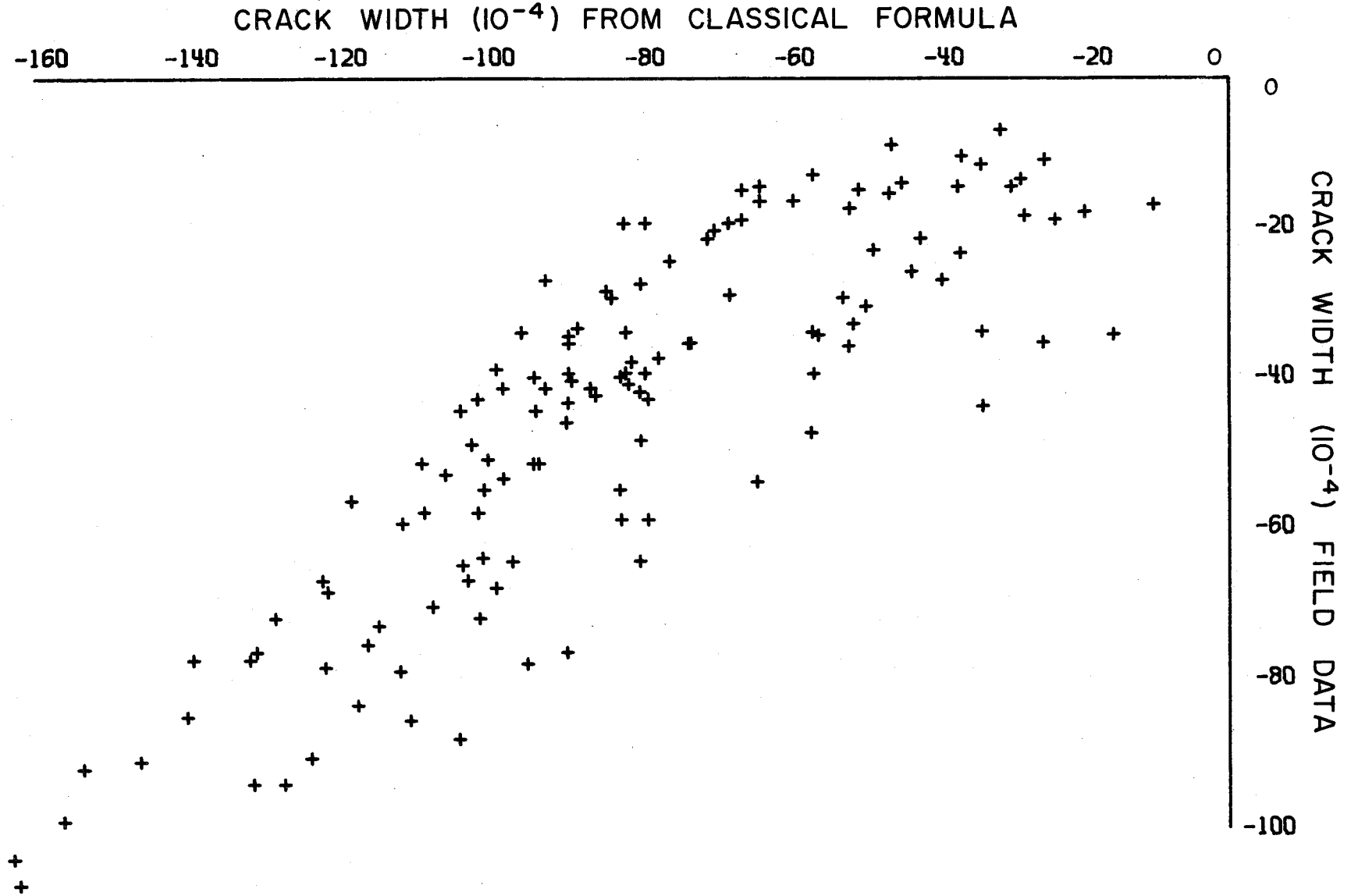

MEASURED CRACK WIDTHS COMPARED TO CALCULATIONS BY CLASSICAL FORMULA

Figure 5.6

$$CDx = -(\bar{X}\ (\Delta Z) + \bar{X}\ \alpha_c\ \Delta T) \quad \ldots\ldots\ldots\ (5)$$

The models are:

Model No.

D11 $\quad Dx = \dfrac{CDx}{e^{P}} \quad \ldots\ldots\ldots\ (6)$

D21 $\quad Dx = \dfrac{CDx}{1 + P} \quad \ldots\ldots\ldots\ (7)$

DK1 $\quad Dx = \dfrac{CDx}{e^{K_1 P}} \quad \ldots\ldots\ldots\ (8)$

DK2 $\quad Dx = \dfrac{CDx}{1 + K_2 P} \quad \ldots\ldots\ldots\ (9)$

Where:

Dx = crack width, inch.

P = per cent longitudinal steel

CDx is defined in Equation (5)

K_1, K_2 are unknown constants

The first two models shown in Equations (6) and (7) are term-wise self-explanatory. The per cent steel term is used as a modification in two different forms. In the first, it is a power of "e" and in the second, it is added to a

whole number. Both of these models indicate logically that a higher percentage of steel would result in a smaller crack width.

The third and fourth models are modifications of the first two in that the per cent steel is multiplied by a constant. The constant "K" was determined by solving the following equation for K_1.

$$Dx = \frac{CDx}{e^{K_1 P}}$$

$$K_1 = \frac{\log_e (CDx/Dx)}{P}$$

Where:

Dx = field crack width measurement

CDx = calculated value by Equation (5)

P = respective per cent steel

For each data point from all six sections, a K_1 was calculated. The average for all positive, non-zero values of this K_1 was then substituted into the regression model shown in Equation (8).

The "K_2" term was determined by solving the following equation for K_2 for each data point:

$$Dx = \frac{CDx}{1 + K_2 P}$$

$$K_2 = \frac{CDx - Dx}{Dx \cdot P}$$

Where: All terms are as previously defined. Again, all positive, non-zero values of K_2 were averaged and the average K_2 was then substituted into Equation (9).

Computations for crack width using all data in the "classical" formula is presented in Figure 5.7. The four models shown in Equations (6) through (9) were evaluated using regression techniques to determine the remaining constants from the data. Table 5.1 shows the regression constants and the statistical correlation for each model. In Figures 5.8 through 5.11, the calculated and the measured crack widths are plotted for each of the four models. The line of equality is shown together with the regression line on each particular graph.

From Table 5.1 it can readily be seen that the four models show about the same correlation. A study of crack width and per cent steel indicates that all four of the models fit the data in generally the same pattern.

Table 5.1

REGRESSION CONSTANTS AND STATISTICS OF CORRELATION

Model	C	D	Coefficient of Determination	Coefficient of Correlation	Standard Standard Error of Estimate
D11	0.00064	0.87560	0.7850	0.8860	0.00094
D21	0.00064	0.79842	0.7852	0.8861	0.00094
DK1	0.00064	1.10713	0.7857	0.8864	0.00094
DK2	0.00064	1.20985	0.7850	0.8860	0.00094

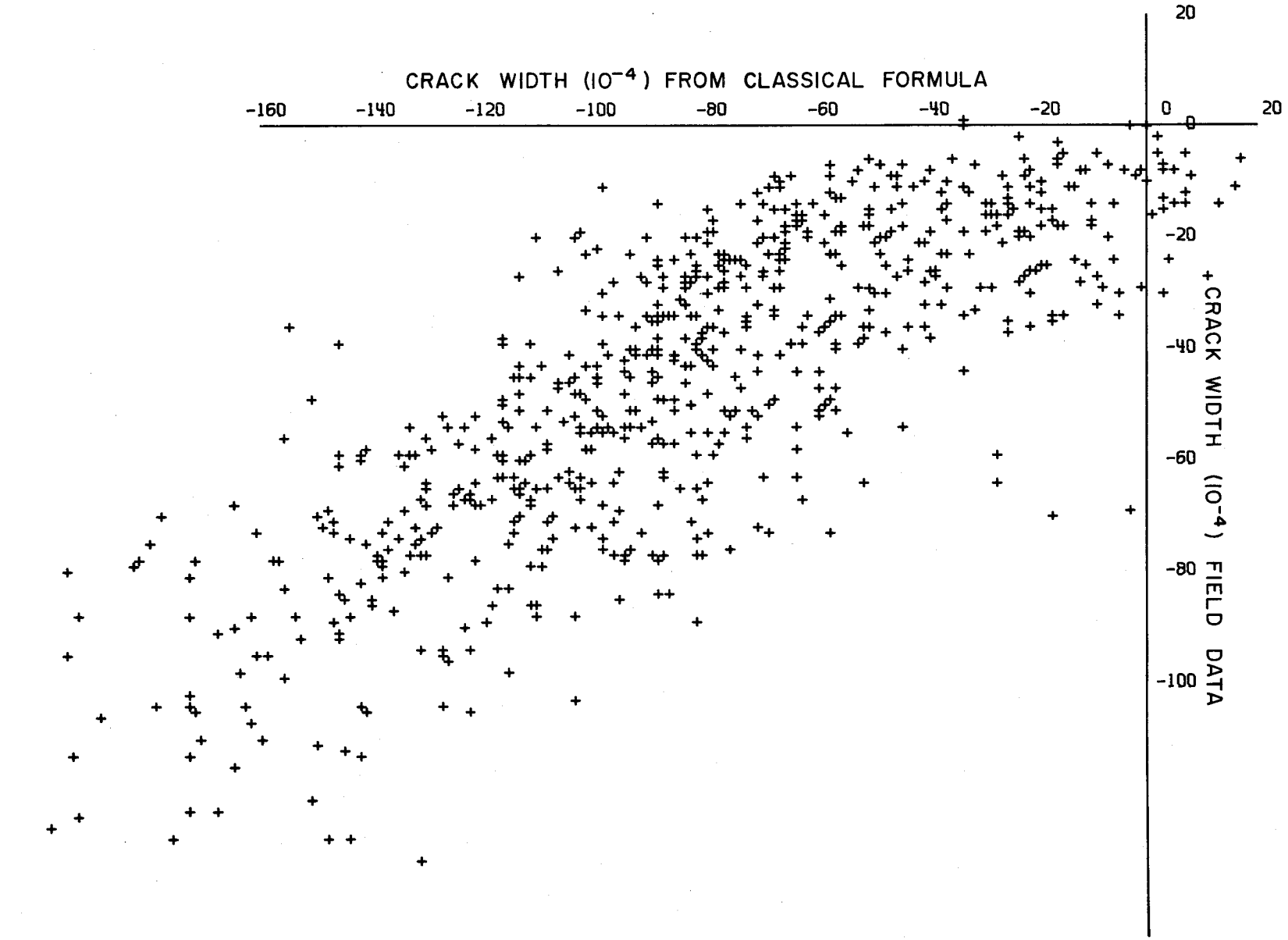

COMPARISON OF DATA TO CLASSICAL FORMULA

Figure 5.7

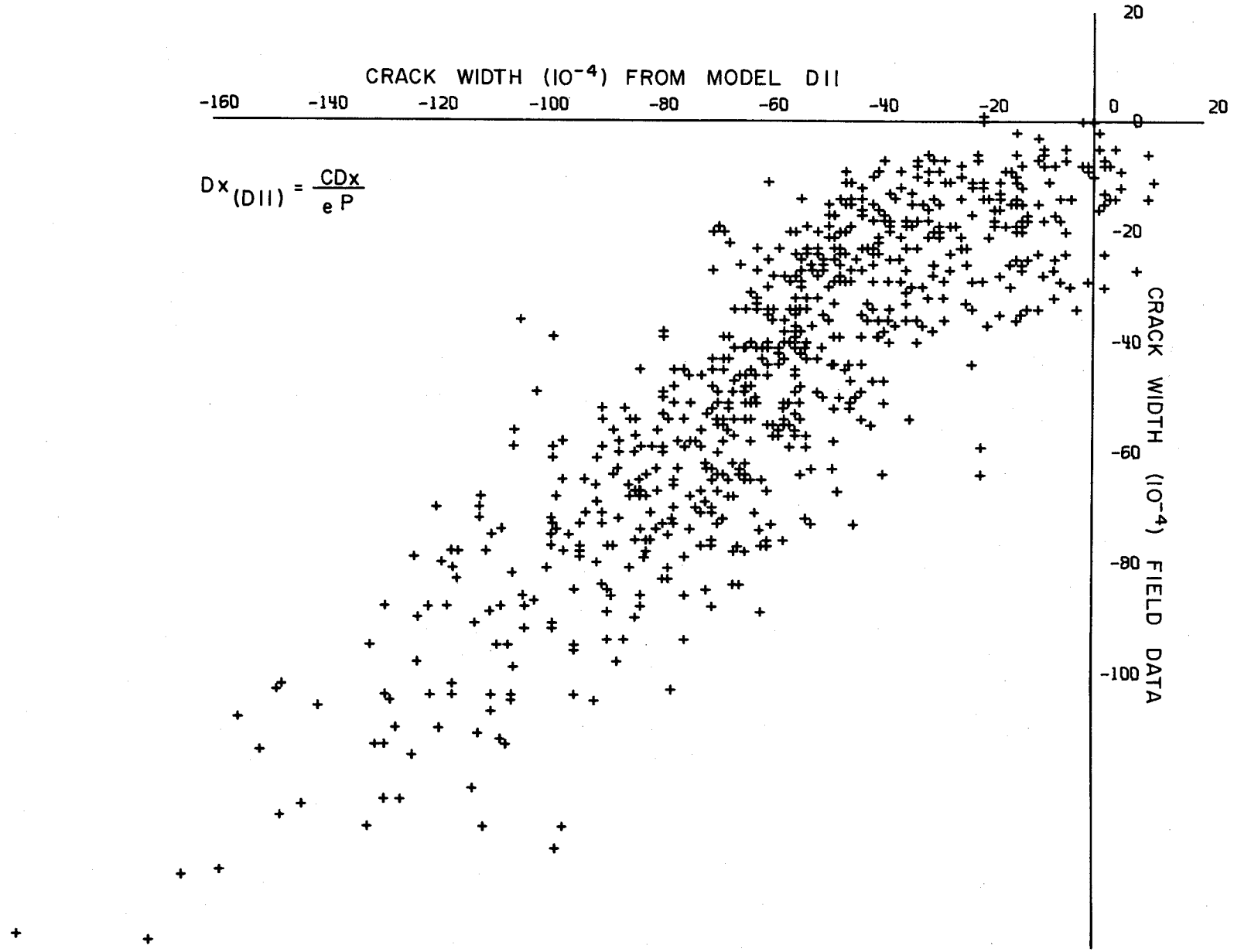

COMPARISON OF DATA WITH MODEL DII

Figure 5.8

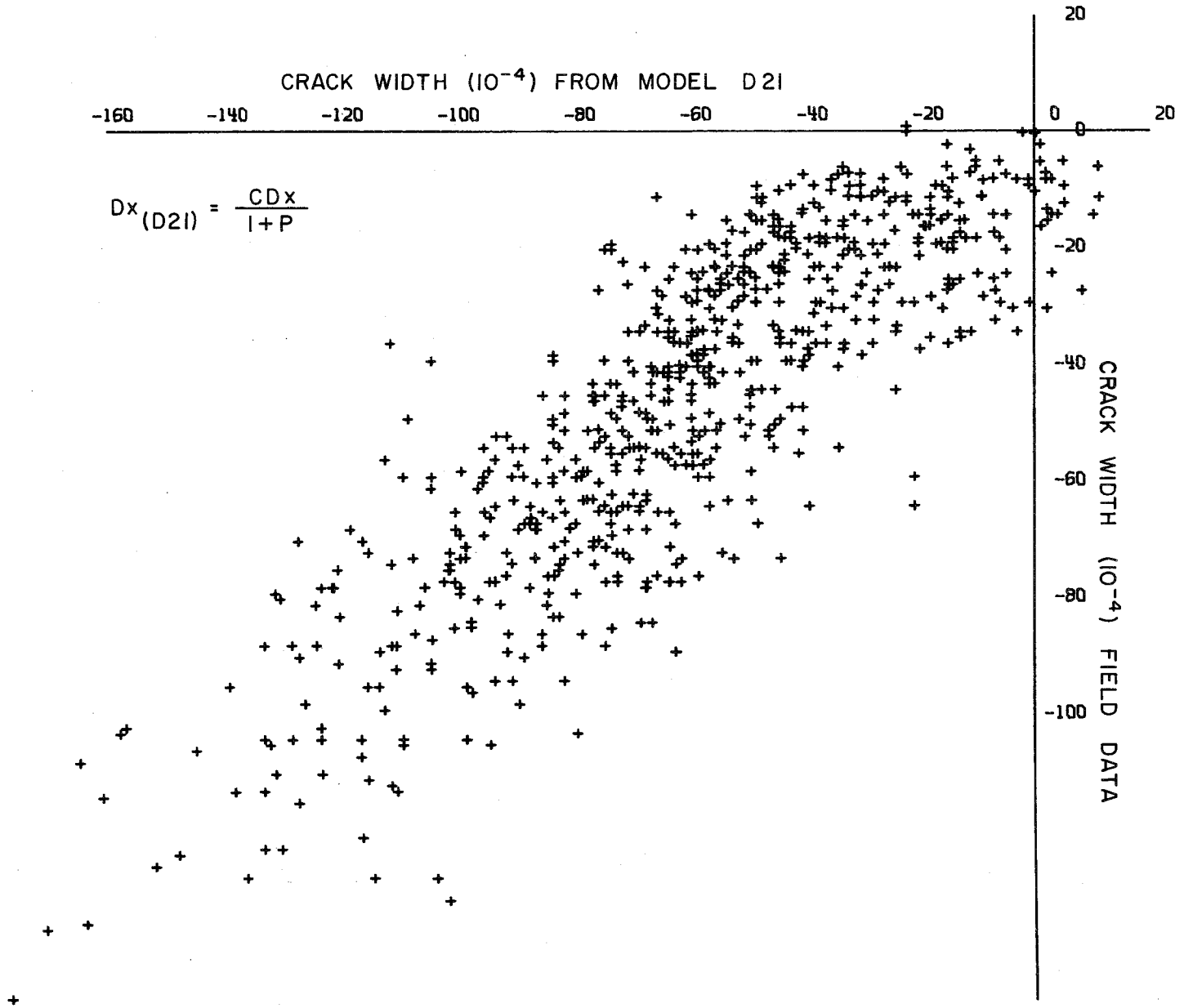

COMPARISON OF DATA WITH MODEL D 21

Figure 5.9

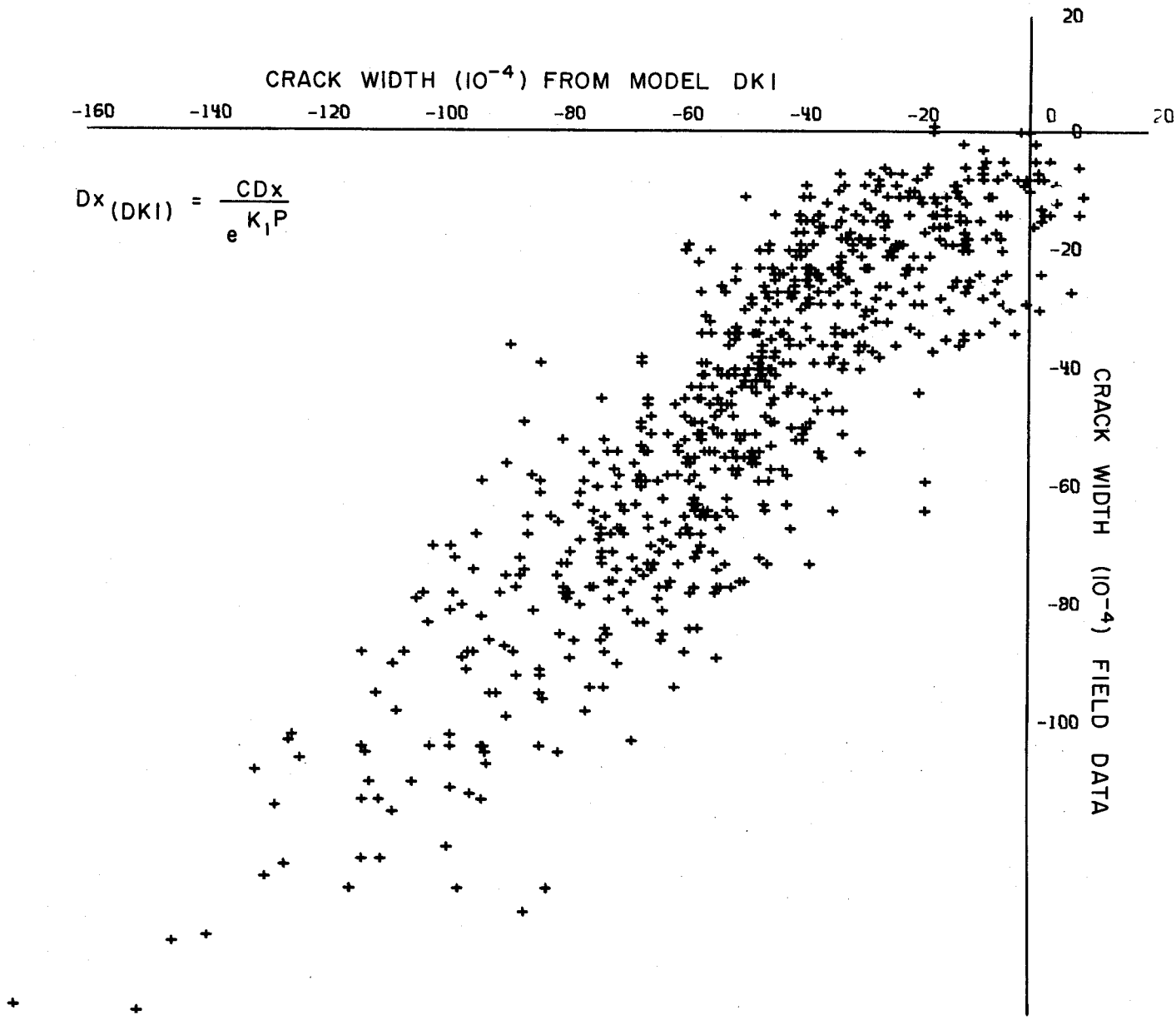

COMPARISON OF DATA WITH MODEL DK I

Figure 5.10

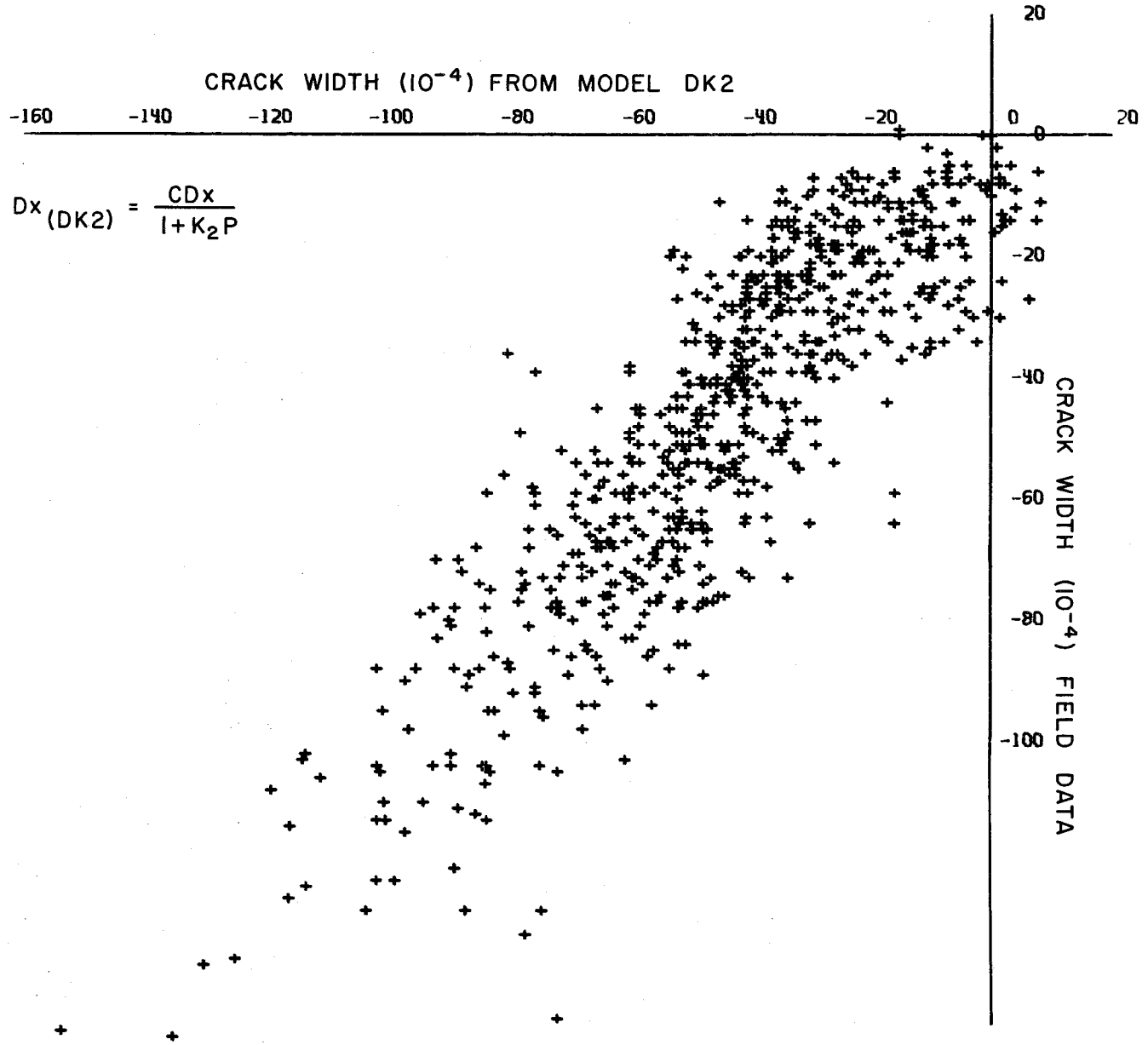

COMPARISON OF DATA WITH MODEL DK 2

Figure 5.11

Figure 5.12 shows the effect of per cent steel on crack width as predicted by each of the four models. The four models have the same general graphical form. The range of the per cent steel data was from 0.3 to 0.5 per cent.

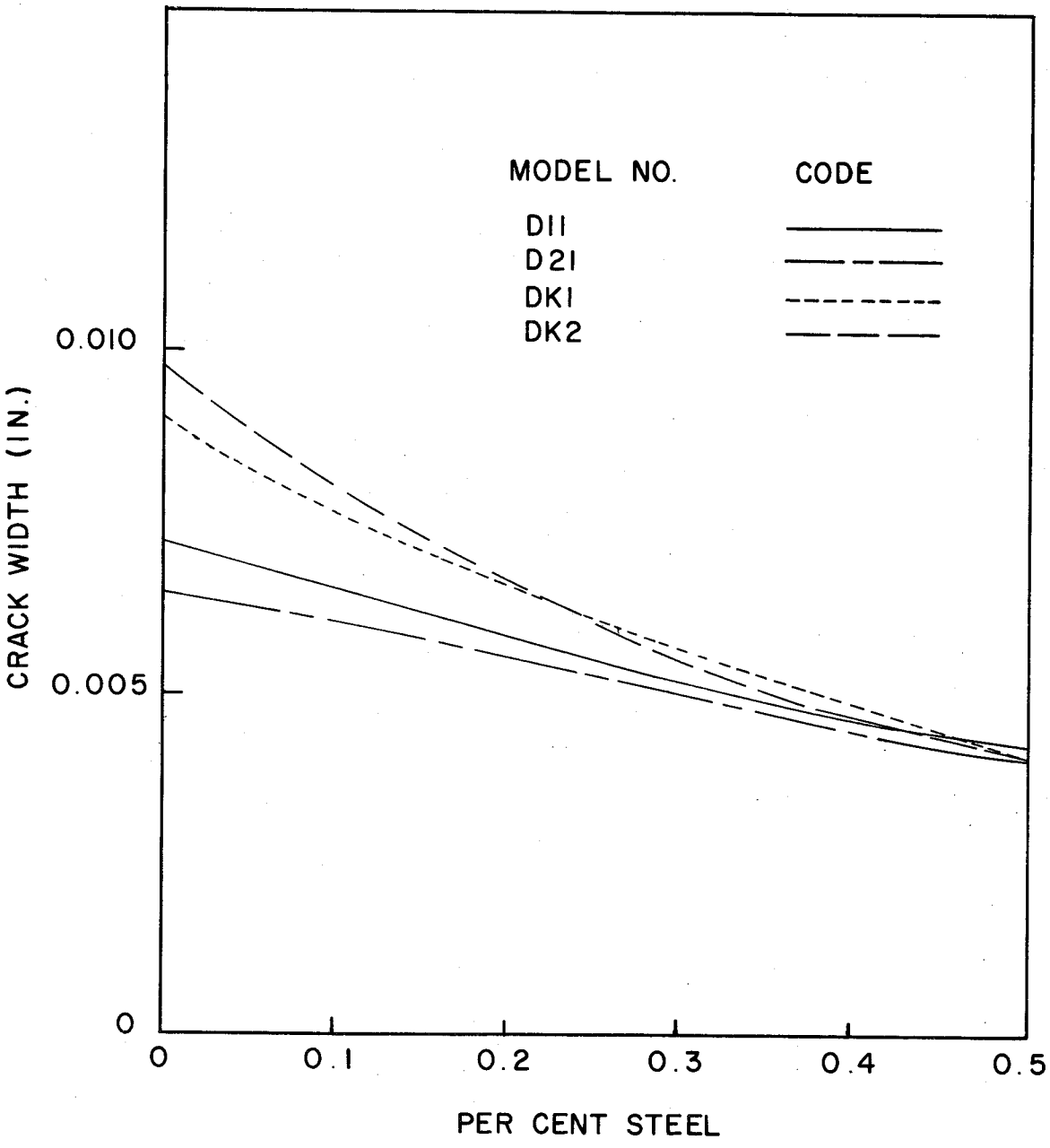

FIGURE 5.12

EFFECT OF PER CENT STEEL

ON CRACK WIDTH

VI. DISCUSSION OF RESULTS

The stresses in the longtitudinal steel caused by temperature change and shrinkage have been analyzed from a logical standpoint and also in coherence with theoretical concepts. The crack width or concrete movement data has also been analyzed in this same manner. The empirical equations presented are based on the data and the best analysis that could be made.

The empirical equations will serve as tools in new design methods based on performance of existing in-service pavements. These equations can be combined with equations for deflection and serve as the basis for the design of CRCP. Another report on this research project will cover whatever design concepts will arise from this study of stresses and crack widths.

The equations are based on data from six test sections on one pavement and therefore are limited. Chapters IV and V covered the boundary conditions on the parameters displayed in each respective empirical equation.

Three empirical equations were developed for stress in the steel. It is believed that the second modification as it is referred to in Chapter 4 is the best of the three analyses. It is the simplest in form and according to the statistics, it describes the correlation equally well as do the first two models.

When the pavement test sections were two years and four months old, the present serviceability index (PSI) was obtained for each section. The PSI was obtained using the CHLOE profilometer. The PSI values for each section are shown in Table 6.1. The degree of spalling of the transverse volume change cracks was evaluated qualitatively for each section. The lightweight concrete is in excellent condition. The conventional concrete has experienced some light to moderate spalling. The sections showing this are indicated in Table 6.1. Stains on the pavement surface at the cracks were also observed. The subbase is a non-errosive cement stabilized oyster shell layer.

Performance wise the test sections look good to the date of this report.

TABLE 6.1

CONDITION OF TEST SECTIONS

Section	Spalling	PSI	Stains on Cracks	Longitudinal Cracking
1	Moderate	3.70		Yes
2	Minor	3.75		
3	Minor	4.07		Yes
4		3.97	Yes	
5	Minor	3.90		
6	Moderate	3.47	Yes	
7	Moderate	4.16	Yes	Yes
8		3.97		
9	Minor	3.48		
10		3.48		
11		3.76		

VII. CONCLUSIONS

This investigation of an experimental continuously reinforced concrete pavement warrants the following conclusions:

1. Temperature stresses in longitudinal reinforcement are a direct function of concrete's modulus of elasticity and the thermal coefficient of concrete.

2. The combination of shrinkage in the concrete and the concrete modulus of elasticity have a pronounced effect on the stress in the steel.

3. Steel stress is an inverse function of the per cent longitudinal steel.

4. The steel stress is directly related to the crack spacing of the concrete.

5. The developed empirical equation can be used to predict steel stresses with reasonable accuracy within its interpolative range if accurate values of all the parameters are known.

6. A curvalinear relationship exists between crack width in the concrete pavement and temperature change. This observation is due to the interaction of attempted concrete movement and restraint by the steel.

7. The entire slab length between volume change cracks contributes to the crack width, thus the actual crack spacing is the effective crack spacing on this project.

8. Small changes in the coefficient of thermal expansion of the concrete have a direct effect on the crack width or movement.

9. The shrinkage of the concrete affects movement in a direct relation.

10. The crack width is directly related to the slab length or crack spacing.

11. The crack width is an inverse function of the per cent of longitudinal steel.

12. The parameters studied effecting crack width or concrete movement can be correlated into an empirical equation to effectively predict crack widths in CRCP.

13. Crack widths as measured in this investigation give a true representation of the movement of the concrete in the upper two inches of the slab rather than surface crack widths as have been studied in previous investigations. Studies on another experimental pavement indicated the two were approximately equal within the measuring capabilities.

The analysis of steel stresses which is the basis for some of the above conclusions was based on data taken during the first eight days of the pavement's life.

B I B L I O G R A P H Y

1. McCullough, B. F. and Ledbetter, Wm. B., "LTS Design of Continuously Reinforced Concrete Pavement", Journal the Highway Division, Proceedings of the American Society of Civil Engineers, December 1960, Paper 2677.

2. Shelby, M. D. and McCullough, B. F., "Experience in Texas with Continuously Reinforced Concrete Pavement", Highway Research Board Bulletin 274, Washington, D. C., National Academy of Sciences, January 1960.

3. Shelby, M. D. and McCullough, B. F., "Determining and Evaluating the Stresses in an In-Service Continuously Reinforced Concrete Pavement", Highway Research Record No. 5, Washington, D. C., National Academy of Sciences, January 1963.

4. McCullough, B. F., "Development of Equipment and Techniques for a Statewide Rigid Pavement Deflection Study", Research Report No. 46-1, Texas Highway Department, January 1965.

5. McCullough, B. F., and Treybig, Harvey J., "Determining the Relationship of Variables in Deflection of Continuously Reinforced Concrete Pavement", Highway Research Record No. 131, Washington, D. C., National Academy of Sciences, January 1966.

6. Shelby, M. D. and Ledbetter, W. B., "Experience in Texas with Terminal Anchorage of Concrete Pavement", Highway Research Board Bulletin 332, Washington, D. C., National Academy of Sciences, January 1962.

7. Standard Specifications for Road and Bridge Construction, Texas Highway Department, 1962.

8. McCullough, B. F., "The Early Service Life Characteristics of a Continuously Reinforced Concrete Pavement in Comal County, Texas", Research Report No. 62-4, Texas Highway Department, 1962.

9. Jones, T. R., Hirsch, T.J., and Stephenson, "The Physical Properties of Structural Quality Lightweight Aggregate Concrete", RP-7, Texas Transportation Institute, August 1959, pp. 16-21.

10. Jones, T.R. and Hirsch, T. J., "The Physical Properties of Concrete at Early Ages", RP-19, Texas Transportations Institute, August 1961.

11. Odman, Sven T.A., "Crack Formation Due to Shrinkage of Reinforced Concrete", Rilem Bulletin No. 9, New Series, December 1960, pp. 100-109.

APPENDIX A

MODULUS OF ELASTICITY OF REINFORCING STEEL

SUMMARY OF RESULTS IN USING THE SR-4 ELECTRICAL STRAIN GAGES VS. MECHANICAL GAGE TO OBTAIN THE MODULUS OF ELASTICITY OF REINFORCING STEEL

MECHANICAL GAGE

Bar #1 with a yield of 64,052 psi and an ultimate of 109,150 psi was taken up in 3000 # increments to 15,000 # three times. Then taken to failure with the following results:

$$E = 30.8 \times 10^6 \text{ psi}$$
$$= 30.2 \times 10^6 \text{ psi}$$
$$= 30.6 \times 10^6 \text{ psi}$$

$$\text{Avg. } E = \frac{91.6}{3} = 30.53 \times 10^6 \text{ psi}$$

Bar #2 with a yield of 64,705 psi and an ultimate of 109,803 psi was taken in 1000 # increments to 12,000 # then to ultimate with the following results:

$$E = 30.1 \times 10^6 \text{ psi}$$
$$= 30.0 \times 10^6 \text{ psi}$$
$$= 30.8 \times 10^6 \text{ psi}$$

$$\text{Avg. } E = \frac{90.9}{3} = 30.3 \times 10^6 \text{ psi}$$

Strain gages were placed on opposite sides of the bar and loaded in increments of 1000 # to 12,000 #. This bar was of the same batch as bars #1 and #2 above, but was turned down to an area of 0.256 sq. in. so the SR-4 gages could be attached. The load was

then applied and let off two times and the data plotted for both runs on the same sheet. The plots for both runs fell on the same line and the modulus of elasticity for each gage is as follows:

$$E = 31.9 \times 10^6 \text{ psi}$$
$$\underline{= 28.4 \times 10^6 \text{ psi}}$$

$$\text{Avg. } E = \frac{60.3}{2} = 30.15 \times 10^6 \text{ psi}$$

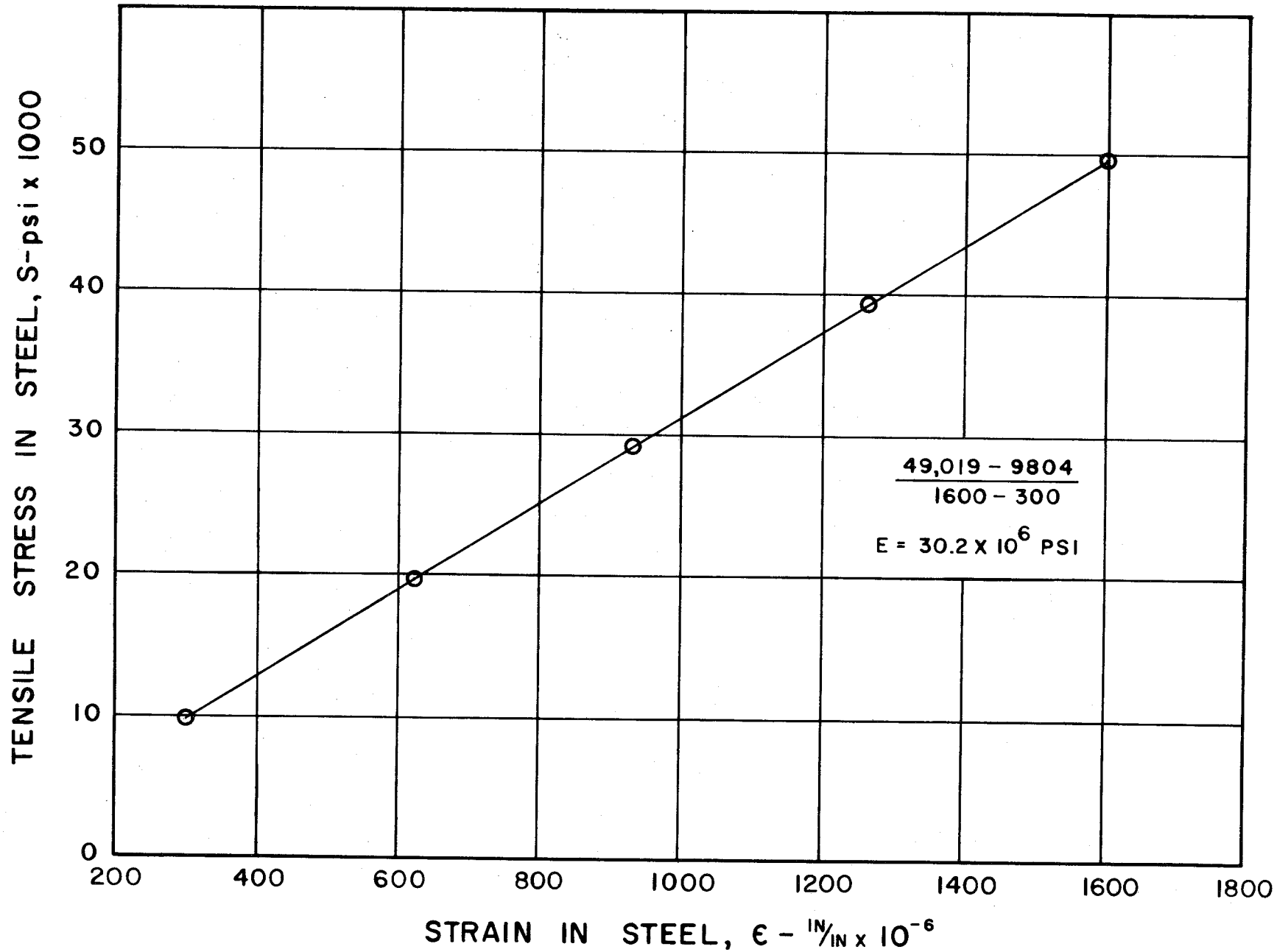

TYPICAL PLOT USED FOR OBTAINING STEEL MODULUS

FIGURE A.1

APPENDIX B

LABORATORY TESTING FOR EXPERIMENTAL CRCP

LABORATORY TESTING FOR EXPERIMENTAL CRCP RESEARCH PROJECT IN HARRIS COUNTY

Modulus of Elasticity

Test specimens were the same as those prepared for the determination of the compressive strength of concrete, Test Method Tex 418-A, and were fabricated and cured in like manner.

Four test specimens were made for each test period of 3, 7, 14, and 28 days. Compressive strength and Modulus of Elasticity determinations were obtained at the same time on the specimens.

Thermal Coefficient

There was no standard procedure for the performance of this test and various references indicated that the thermal coefficient of expansion of a particular concrete appeared to have different values when the concrete was at different stages of saturation with water.

One method of making this determination was by making extra shrinkage test specimens and subjecting these specimens to the desired temperature changes at the selected test periods. Linear changes were measured by means of a length comparator. These specimens were cured by the method selected as the most applicable for their use.

Forms for this test were made in accordance with ASTM Designation C 157. The specimens were not destroyed when making this determination and were used throughout the test cycle. This required only one set of test specimens for each test condition.

Tensile Strength

It was not certain if this test was to be made on the cement or the concrete. If it was intended that this test be made on the concrete then Test Method Tex-426-A should have been followed.

Forms for making test specimens of concrete were made in accordance with the above test method and in sufficient numbers for 3, 7, 14 and 28 day test specimens for each test condition.

Flexural Strength

Test Method Tex-420-A outlines the procedure for fabricating and testing simple single beams with center point loading to determine the flexural strength of the concrete.

Volume Change (Lineal Shrinkage)

Test Method Tex-422-A outlines the procedure for making and testing the specimens for this determination with the exception that the test molds should be constructed to

conform with the mold specifications in ASTM Designation C 157.

The test specimens were not destroyed at test and were used for each test period. This required only one set of test specimens for each test condition.

Shrinkage test specimens are normally moist cured for the first 28 days and then stored dry at room temperature with measurements being taken monthly and semi-annually until the end of the investigation is reached. The extent of testing as outlined by D-8 indicates that only the first 28 days is under study; therefore, it was recommended that measurements be made at the 3, 7, 14 and 28 day periods.

Cement Fineness

Routine samples of cements used were submitted to this Division for the determinations requested.

Bond Strength

Test Method Tex-425-A outlines a method for determining the apparent bond strength. This method makes use of standard cylinder molds, which are readily available, for making the test specimens.

Many of the test requested are of such nature that normally the samples are prepared in the laboratory where

greater care can be taken to ensure that the test specimens will not be damaged during curing or excessive moving. Particularly sensitive to damage are the test specimens for the determination of the Thermal Coefficient of Expansion, Tensile Strength and Shrinkage. These test specimens can be made and tested, but it should be noted that the possibilities of damaging the specimens at the job site or in transportation to this laboratory testing are quite numerous.

A final summation of the required forms per test site or test condition were:

Standard Cylinder Molds	28	
Standard Beam Molds	12	
Lineal Shrinkage Molds	6	(to be made)
Tensile Strength Molds	12	(6 on hand, remainder to be made)

The test specimens must remain in the mold for a minimum of 24 hours; therefore, if more than one section is to be tested per day, or if more than 24 hours are required prior to removal of the forms with a schedule for making new specimens each day, then the above figures must be multiplied by a number sufficient to allow for these conditions.

APPENDIX C

THEORETICAL STEEL STRESS FORMULA

THEORETICAL STEEL STRESS FORMULA FOR HARRIS COUNTY CRCP STUDY

In connection with the enumerated project, there is a need for deriving a theoretical formula for predicting stresses in the steel due to volumeteric changes. The formula can then be correlated with the data to obtain modifying coefficients. Since the greatest steel stresses are experienced at a crack, this will be the condition considered for analysis.

Stress Producing Factors

The two primary factors producing volume change or attempted volume change are concrete shrinkage and temperature change. A temperature change will produce an internal stress in the steel and the concrete. The restraint offered by the steel to the concrete attempted relief movement at the crack will produce additional steel stresses. This hypothesis can be expressed as follows:

$$S_s = S_I + S_c \quad \ldots\ldots\ldots\ldots\ldots\ldots (1)$$

Where:

S_s = Total stress in steel

S_I = Internal stresses developed within the steel due to temperature change

S_c = Stresses developed in the concrete due to restraint of concrete volumetric changes

Internal Steel Stresses

The internal stresses developed within the steel can be expressed by combining the basic linear deformation relationship and Hooke's Law.

$$S_I = \alpha_s \Delta T \; E_s \quad \ldots\ldots\ldots\ldots\ldots\ldots \quad (2)$$

Where:

α_s = Thermal coefficient of steel

ΔT = Temperature change

E_s = Modulus of elasticity of steel

Steel Stresses Due To Concrete Volume Changes

The stresses developed in the steel due to concrete volume changes are in essence the net difference in the theoretical movement due to environmental conditions and the actual relief movement experienced by the concrete. Since stress is a mathematical derivation, the stresses in the concrete and steel cannot be added or subtracted directly. Any "free body" balancing between the two materials must be done in terms of force.

The actual force in the concrete at the crack is equal to the theoretical force in the concrete due to volume change minus the frictional resistance offered by the subbase and the relief force developed due to concrete movement. This may be expressed as follows:

$$F_c = F_{tc} - F_{mc} - F_{fc} \quad \ldots\ldots\ldots\ldots \quad (3)$$

Where:

F_c = Actual or net force in the concrete

F_{tc}= The theoretical force that would be developed in the concrete if fully restrained

F_{mc}= The relief movement experienced by the concrete. (In the case for the experiment, the measured movement.)

F_{fc}= The frictional resistance force offered by the subbase

Theoretical Force. The theoretical force within the concrete can be expressed by the basic linear deformation relationship and Hooke's Law:

$$F_{tc} = \alpha_c \Delta T \; E_c A_c \quad \ldots\ldots\ldots\ldots\ldots\ldots \quad (4)$$

Where:

α_c = Thermal coefficient of concrete

E_c = Modulus of elasticity of concrete

A_c = Cross sectional area of concrete

Relief Force. The force developed due to movement of the concrete is as follows:

$$F_{mc} = \frac{\Delta X}{\overline{X}} E_c A_c \quad \ldots\ldots\ldots\ldots\ldots\ldots \quad (5)$$

Where:

ΔX = Measured concrete movement

$\overline{X}$ = Effective average crack spacing

Frictional Force. Goldbeck, in his study of frictional tests on concrete found that the frictional force was a function of the concrete movement and the concrete weight. Basically the expression is as follows:

$$F_{fc} = B\,\Delta X^{n}\,A_c\,\bar{X}\,W \quad \ldots\ldots\ldots\ldots\ldots\ldots\ldots\ldots \quad (6)$$

Where:

B,n = Constants depending on frictional resistance of subbase

W = Unit weight of concrete, #/in^3

By combining equations (3), (4), (5), and (6) the following equation is obtained:

$$F_c = \alpha_c \Delta T\, E_c A_c - \frac{\Delta X}{\bar{X}}\, E_c A_c - B\Delta X^{n} A_c\, \bar{X}\, W \quad \ldots \quad (7)$$

Since the pavement slab is in static equilibrium at any given time period, the net force in concrete is equal to the developed force in the steel. By making this substitution in equation (7) and dividing by steel area to convert to stress the following is derived:

$$S_c = \frac{\alpha_c \Delta T\, E_c A_c - \frac{\Delta X}{\bar{X}}\, E_c A_c - B\Delta X^{n} A_c\, \bar{X}\, W}{A_s} \quad \ldots \quad (8)$$

Combination of Stress Producing Factors:

By substituting equations (2) and (8) into equation (1) and combining terms an expression for steel stress is obtained:

$$S_s = \alpha_s \Delta T E_s + \frac{\alpha_c \Delta T E_c}{P} - \frac{\Delta X E_c}{\bar{X} P} - \frac{B \Delta X^n \bar{X} W}{P} \quad . . (9)$$

If a suitable expression for ΔX is obtained in the concrete analysis, it can be substituted in equation (9).

Assumptions

1. The pavement slab is assumed to be in static equilibrium at any given instant.

2. External stresses developed from such factors as wheel loads are not considered in this analysis. The stresses are assumed to be the result of the volume change properties of the steel and concrete.

3. The volume changes induced by moisture fluctuations are not considered in this analysis.

4. Hooke's Law is applicable to the concrete.

APPENDIX D

THEORETICAL CONCRETE MOVEMENT FORMULA

THEORETICAL CONCRETE MOVEMENT FORMULA

FOR

HARRIS COUNTY CRCP STUDY

Odman in his treatise on "Crack Formation due to Shrinkage of Reinforced Concrete" derived the following formula for predicting crack width.[11] This formula is for shrinkage only, excluding temperature.

$$w = \frac{\frac{mk}{4} \cdot \frac{d}{r}}{1 + m\mu + a_i mk\mu \frac{\tau_e}{K_{ct}}} E_{sh} \cdot \cdot \cdot \cdot \cdot \cdot \cdot \cdot \cdot \cdot \cdot \quad (1)$$

Where:

w = Crack width

k,m = Unknown coefficient

d = Bar diameter

μ = Ratio of reinforcement

a = A dimensionless constant

r = Coefficient of bond properties

τ_e = Effective bond stress

K_{ct} = Concrete tensile strength

Changing the nomenclature the above equation can be written as:

$$DX_Z = \frac{A_o \frac{d}{4r}}{1 + A_2 P + A_3 P \frac{u}{S'_c}} Z \qquad \ldots\ldots\ldots\ldots\ldots\ldots\ldots (2)$$

Where:

A_o = Unknown constant (mk)

d = Bar Diameter

r = Coefficient of bond properties

A_2 = Unknown constant (m)

P = Steel area to concrete area ratio (μ)

A_3 = Unknown constant ($a_1 mk$)

u = Effective bond stress

S'_c = Concrete tensile strength

Z = Shrinkage of concrete

Since Odman's formula does not take temperature change into account, the formula must be altered to account for crack movements resulting from temperature variations. The crack width variations due to temperature changes should be additive to that predicted by shrinkage, since a change

in crack width can be the result of either shrinkage or temperature change.

Theoretical derivations have been made that predict end movement of a specimen due to temperature changes. In its simplest form the formula is as follows:

$$\Delta L = L \alpha \Delta t \quad . . . . . \quad (3)$$

Where:

ΔL = Change in unit length

L = Length of specimen

α = Thermal coefficient of expansion for material

Δt = Temperature differential

Studies on CRCP in connection with this experiment indicate that the movement at a crack follows the basic relation:

$$DX_T = M \bar{X} \alpha \Delta t_m \quad . . . . . \quad (4)$$

Where:

DX_T = Change in crack width due to temperature changes

$\bar{X}$ = Effective crack spacing (part of slab segment actually experiencing movement)

M = Correlation constant (includes subbase friction)

Δt_m = Change in temperature.

Studies have also indicated that the movement is inversely proportional to subbase friction. Since the movement would follow the theoretical if the subbase friction term were zero, the friction coefficient must be added to a whole number. The equation takes the following form:

$$DX_T = \frac{A_4 \bar{X} \alpha (t_o - t_n)}{(K+1)} \quad \ldots\ldots\ldots\ldots\ldots\ldots \quad (5)$$

Where:

K = Subbase coefficient of friction

t_o = Reference temperature

t_n = Temperature at any time

It is logical that the amount of movement due to temperature change would be inversely proportional to the amount of reinforcing steel in the slab. The steel to concrete area ratio would also have to be added to a whole number. The equation now takes the following form:

$$DX_T = \frac{A_4 \bar{X} \alpha (t_o - t_n)}{(K+1)(P+1)} \quad \ldots\ldots\ldots\ldots (6)$$

The crack width at any given time would be a net combination of the effects of temperature and shrinkage.

$$DX = DX_Z + DX_T \quad \ldots\ldots\ldots\ldots (7)$$

Substituting Equations (2) and (6) into (7) the following theoretical model for crack width is obtained:

$$DX = \frac{A_o d/4r}{1 + A_2 P + \frac{A_3 P}{S'_c}} \cdot Z + \frac{A_4 \bar{X} \alpha (t_o - t_n)}{(K+1)(P+1)} \quad \ldots\ldots\ldots\ldots (8)$$

APPENDIX E

DATA SHEETS

STEEL STRESS DATA SHEET
PROJECT 1-8-63-46

1	2	3	4

STEEL STRESS STUDY | 5 |
|---|
| |

TEST SECTION NO. | 6 | 7 | 8 |
|---|---|---|
| | | |

DATE	9	10	11	12	13	14

	GAUGE 1	GAUGE 2	GAUGE 3	GAUGE 4	GAUGE 5	GAUGE 6	GAUGE 7	GAUGE 8	GAUGE 9	GAUGE 10	SLAB TEMP.		TIME
											START	FINISH	
RUN NO.	15 16 17 18 19	20 21 22 23 24	25 26 27 28 29	30 31 32 33 34	35 36 37 38 39	40 41 42 43 44	45 46 47 48 49	50 51 52 53 54	55 56 57 58 59	60 61 62 63 64	65 66 67 68 69	70 71 72 73 74	75 76 77 78
1													
2													
3													
4													
5													
6													
7													
8													
9													
10													
11													
12													
13													
14													
15													
16													
17													
18													
19													
20													
21													
22													
23													
24													
25													

CONCRETE MOVEMENT DATA SHEET
PROJECT 1-8-63-46

1	2	3	4

CONCRETE MOVEMENT STUDY

5

TEST SECTION NO.

6	7	8

DATE

9	10	11	12	13	14

CARD NO.

15
1

	TIME	SLAB TEMP.		ZERO READING		GAUGE PLUG READING									
		START	FINISH	START	FINISH	1-2	2-3	3-4	4-5	5-6	6-7	7-8	8-9	9-10	10-11
RUN NO.	16 17 18 19	20 21 22 23 24	25 26 27 28 29	30 31 32 33	34 35 36 37	38 39 40 41	42 43 44 45	46 47 48 49	50 51 52 53	54 55 56 57	58 59 60 61	62 63 64 65	66 67 68 69	70 71 72 73	74 75 76 77
1															
2															
3															
4															
5															
6															
7															
8															
9															
10															
11															
12															
13															
14															
15															
16															
17															
18															
19															
20															
21															
22															
23															
24															
25															